General Multi-User Distributed Computing

Ali Khalesi

Institut Polytechnique des Sciences Avancées (IPSA), Paris, France ali.khalesi@ipsa.fr

Abstract

This work develops a unified learning- and information-theoretic framework for distributed computation and inference across multiple users and servers. The proposed General Multi-User Distributed Computing (GMUDC) model characterizes how computation, communication, and accuracy can be jointly optimized when users demand heterogeneous target functions that are arbitrary transformations of shared real-valued subfunctions. Without any separability assumption, and requiring only that each target function lies in a reproducing-kernel Hilbert space associated with a shift-invariant kernel, the framework remains valid for arbitrary connectivity and task-assignment topologies. A dual analysis is introduced: the quenched design considers fixed assignments of subfunctions and network topology, while the annealed design captures the averaged performance when assignments and links are drawn uniformly at random from a given ensemble. These formulations reveal the fundamental limits governing the trade-offs among computing load, communication load, and reconstruction distortion under computational and communication budgets Γ and Δ . The analysis establishes a spectral-coverage duality linking generalization capability with network topology and resource allocation, leading to provably efficient and topologyaware distributed designs. The resulting principles provide an information-energy foundation for scalable and resource-optimal distributed and federated learning systems, with direct applications to aeronautical, satellite, and edge-intelligent networks where energy and data efficiency are critical.

Index Terms

Distributed Computing, Bulk Synchronous Parallel (BSP), Distributed Learning, Kernel Methods, Reproducing-Kernel Hilbert Space (RKHS), Computation–Communication Trade-off, Energy-Efficient Artificial Intelligence.

I. Introduction

The increasing complexity of distributed learning, sensing, and computation in modern networked systems demands architectures that can simultaneously balance computation, communication, and

reliability under tight resource constraints such as power and data. As tasks scale across multiple nodes, users, and layers of processing, understanding the fundamental limits of distributed computation becomes essential. The well-known computation—communication tradeoff stands at the heart of distributed computing, serving as a fundamental and unifying principle with profound consequences. This tradeoff manifests as a key limiting factor across diverse distributed computing settings [1]–[7], where computation and communication consistently emerge as the two interdependent bottlenecks governing overall system efficiency. The delicate balance between these resources dictates the achievable performance in virtually all forms of distributed processing and learning, encompassing coded computing, federated learning, and edge inference paradigms.

A further key dimension concerns computational accuracy—that is, the ability to recover the desired tasks of the clients with minimal error or distortion under limited resources. Numerous recent works [8]–[24] have proposed methods to improve this accuracy, typically by introducing approximate or randomized computation techniques.

While classical coded distributed computing frameworks were originally designed around finite-field algebraic codes, such as Reed-Solomon and polynomial-based constructions, their applicability to modern large-scale learning and inference systems remains limited. These algebraic approaches rely on exact recovery over discrete alphabets and are thus ill-suited for real-valued, noisy, and inherently approximate computations that characterize machine learning and signal processing workloads. Motivated by these limitations, a recent line of research has sought to extend coded computing beyond finite-field algebra to operate directly over the reals, embracing approximate computation as a natural and desirable property. This paradigm shift has inspired the development of Learning-Theoretic Coded Computing [25], which formulates coded computation as a functional optimization problem—allowing encoder and decoder mappings to be learned adaptively from data rather than manually designed using algebraic code constructions. Building on this foundation. follow-up works such as General Coded Computing in a Probabilistic Straggler Regime [26] and General Coded Computing: Adversarial Settings [27] have further extended the framework to analyze convergence properties under stochastic and adversarial uncertainties, respectively. Collectively, these studies mark a paradigm shift—from purely algebraic code design toward learning-driven, real-valued coded computing frameworks capable of handling general computation functions with probabilistic or adversarial disruptions.

In essence, real distributed computing operates at the intersection of three tightly interlinked components—accuracy, communication, and computation. The dynamic interplay among these quantities fundamentally governs the achievable performance of large-scale distributed systems.

In this work, we investigate this interplay within the context of *multi-user distributed computing*, providing a unified framework that captures how computation and communication budgets jointly determine the achievable accuracy across heterogeneous servers, topologies with general non-linear demands.

In particular, our setting here considers a coordinator node that manages N server nodes that must contribute in a distributed manner to the computation of the target functions of K different users, where the target functions can be obtained as a general (not restricted to linear) transformation of at most L output subfunctions (See Fig. 1). The subfunctions are supposed to be computed by the servers. More precisely, we consider that user $k \in \{1, 2, ..., K\}$ demands a function

$$F_k(x) = h_k(f_1(x), f_2(x), \dots, f_L(x)), \qquad x \in \mathcal{X} \subseteq \mathbb{R}^d, \ d \in \mathbb{N},$$

that takes as input L subfunctions, where $h_k(\cdot)$ belongs to the Reproducing Kernel Hilbert Space (RKHS) \mathcal{H}_K induced by a bounded, shift-invariant kernel $K(\cdot,\cdot)$. This general formulation captures a wide range of admissible target functions, including linear, polynomial, and smooth nonlinear mappings. For instance, under a linear kernel $K(u,v)=u^{\top}v$, the user functions reduce to linear combinations of the subfunction outputs (Exactly the cases investigated in [8], [28]–[30]); under a polynomial kernel $K(u,v)=(1+u^{\top}v)^q$, the user functions encompass all multivariate polynomials of degree up to q; and under Gaussian or Laplacian kernels, the targets can represent highly smooth or bounded-variation nonlinear transformations. Hence, our framework naturally encompasses both classical linearly-decomposable models and modern nonlinear mappings arising in distributed learning and inference tasks. Furthermore, even when the true user function F_k does not belong exactly to \mathcal{H}_K , our analysis extends to misspecified targets by quantifying an additional approximation (misspecification) error term, ensuring that the main risk bounds remain valid in such general settings.

The above target function formulation serves as an abstraction of distributed matrix—vector and matrix—matrix multiplication [5], [31], distributed gradient coding [32], [33], distributed linear transforms [3], and multivariate polynomial computation [34], all of which fit naturally within the same algebraic structure. Beyond these classical coded computing problems, the framework also encompasses modern distributed learning settings, including federated learning [35], distributed kernel regression and Gaussian-process inference [36], and large-scale ridge regression under communication constraints [37]. Furthermore, it extends naturally to aeronautical and aerospace applications, where distributed sensing and estimation systems—such as UAV swarms, satellite constellations, or formation-flying spacecraft—must jointly estimate or control high-dimensional states from locally

available measurements [38]. Examples include distributed Kalman filtering [39], consensus-based state estimation [38], cooperative trajectory optimization [40], and aerodynamic field reconstruction [41], [42], where each node computes local subfunctions of sensor data, and a coordinator or group of users aggregates these to recover global quantities of interest. Many of these estimation and control laws are linearly separable or admit smooth nonlinear representations in RKHSs, making them directly expressible within our proposed *General Multi-User Distributed Computing (GMUDC)* framework. Consequently, GMUDC not only subsumes existing multi-user distributed computing models as special cases but also provides a unified learning-theoretic foundation for distributed computation and inference across scientific, engineering, and aeronautical domains.

In this work, similar to [8], we assume that the system operates in three sequential phases. In the assignment phase, the subfunctions are allocated to the servers, represented by $A \triangleq (S_1, \ldots, S_N)$, where each $S_n \subseteq \{1, 2, \ldots, L\}$ denotes the set of subfunctions assigned to server n. The assignment must satisfy a computation budget $\Gamma \in \{1, 2, \ldots, L\}$, which specifies the maximum number of subfunctions that can be computed by any single server. In the subsequent computation/encoding phase, each server computes its assigned subfunctions and applies an encoder to generate symbols that are transmitted over error-free links in T shots to the connected users. Finally, in the communication/decoding phase, the encoded symbols are delivered to users according to the network's link structure, which must satisfy the communication budget Δ , representing the maximum number of user links per server. Formally, each server n can communicate with a subset of users $\mathcal{T}_n \subseteq \{1, 2, \ldots, K\}$, and we denote the overall link configuration by $L = (\mathcal{T}_1, \ldots, \mathcal{T}_N)$. After receiving the encoded symbols, each user applies a decoder to reconstruct an approximation \widehat{F}_k of its desired target function F_k .

We measure the performance of each design \mathcal{D} —which consists solely of the encoding and decoding functions of the servers and users—under two complementary regimes. In the first regime, we evaluate the performance for a fixed realization of the computation assignments and communication links (A, L) through the *quenched population risk*, defined as

$$\mathcal{R}(\mathcal{D} \mid \mathsf{A}, \mathsf{L}) = \mathbb{E}_{x \sim \mathbb{P}_X} \left[\frac{1}{K} \sum_{k=1}^K \left\| \widehat{F}_k(x) - F_k(x) \right\|_2^2 \right],$$

where \mathbb{P}_X denotes the input distribution over \mathcal{X} . This quantity captures the reconstruction error of all users given a specific system realization.

The second regime, referred to as the annealed population risk, averages over the randomness of the uniformly distributed computation assignments and communication links, each constrained by the budgets Γ and Δ , respectively:

$$\overline{\mathcal{R}}(\mathcal{D}) \triangleq \mathbb{E}_{\mathsf{A},\mathsf{L}}\big[\mathcal{R}\big(\mathcal{D} \mid \mathsf{A},\mathsf{L}\big)\big]\,,$$

This quantity represents the expected performance of the system over typical random realizations of the network topology. Together, the quenched and annealed population risks provide two complementary characterizations of performance in GMUDC: the former captures *instance-wise* behavior under a fixed network realization, while the latter describes the *average-case* behavior across random topologies. In what follows, we formally define the two optimization problems associated with these performance metrics. The first corresponds to the *quenched design*, where the assignment and link topology are fixed, while the second corresponds to the *annealed design*, which averages performance over random network realizations.

P1 (Quenched design): Given a fixed realization (A, L), the objective is to find encoder and decoder mappings that minimize the quenched population risk:

$$\inf_{\mathcal{D}} \ \mathcal{R}(\mathcal{D} \mid A, L)$$

P2 (Annealed design): In this case, the goal is to minimize the expected (annealed) population risk averaged over all possible random assignments and link configurations:

$$\inf_{\mathcal{D}} \quad \overline{\mathcal{R}}(\mathcal{D}).$$

Here, the design is not conditioned on a specific realization of (A, L), but rather aims to minimize the expected population risk over their random draws. The encoders and decoders may depend on model parameters such as (Γ, Δ, T) and on the data distribution \mathbb{P}_X , but not on any particular instance of the topology.

a) Methods and novelties: Our approach contributes both a new achievable scheme and a new converse tailored to multi-user distributed computing. On the achievability side, we instantiate masked random Fourier feature (RFF) encoders that respect the per-server compute mask of size Γ across T shots, paired with user-wise ridge-regression decoders. This construction yields a (nearly) unbiased Monte Carlo approximation of the kernel on subfunction outputs while explicitly quantifying and controlling the variance introduced by masking and limited fan-out. On the converse side, we develop a spectral-coverage argument that is new in this setting: (i) a spectral lower bound given by the eigen-tail of the kernel integral operator beyond the communicated feature budget, and (ii) a coverage lower bound that enforces a nonzero floor whenever essential subfunction coordinates for any user are not observed by the realized assignment/link topology. In the averaged regime, the coverage penalty decays exponentially in $\gamma N\delta$ (with $\gamma = \Gamma/L$ and $\delta = \Delta/K$), revealing a sharp computational phase transition and establishing tight, learning-theoretic fundamental limits for GMUDC.

b) Quenched fundamental limits (Theorem 1): For any fixed realization (A, L), with high probability we have:

 $\mathcal{R}(\mathcal{D} \mid \mathsf{A}, \mathsf{L}) = \tilde{\mathcal{O}} \left(\frac{B^2}{\gamma \, m_{
m harm}} + \frac{\sigma^2 \, d_{\lambda}}{M} + B^2 \lambda \right)$

where m_{harm} is the harmonic mean of the users' received-feature counts, $d_{\lambda} \triangleq \frac{1}{K} \sum_{k=1}^{K} d_{\lambda,K}$ where $d_{\lambda,K}$ is the effective ridge dimension [43] of each user, B bounds the RKHS norm of each target function ($||F_k||_{\mathcal{H}_K} \leq B$), and $\lambda > 0$ is the ridge-regularization parameter controlling bias-variance tradeoff in the user decoders and M denotes the number of available training samples used to learn the decoder coefficients. Also note that the notation $\widetilde{\mathcal{O}}(\cdot)$ denotes asymptotic upper bounds up to polylogarithmic factors. Moreover, every design obeys the matching (instance-wise) lower bound

$$\mathcal{R}(\mathcal{D} \mid \mathsf{A}, \mathsf{L}) \ = \ \Omega \bigg(\frac{1}{K} \sum_{k=1}^{K} \Big[B^2 \sum_{j > \underline{m}_k(\mathcal{T})} \lambda_j \ \lor \ \varepsilon_{\mathrm{cov},k}(\mathsf{A}, \mathsf{L}) \Big] \bigg)$$

where λ_j are the nonincreasing eigenvalues of the kernel integral operator associated with $K(\cdot, \cdot)$ —representing the spectral complexity of the target functions—and $\underline{m}_k(\mathcal{T})$ denotes the total number of encoded features (scalars) received by user k from all servers under the realized link configuration L . In other words, the risk cannot beat the kernel rank - $\underline{m}_k(\mathcal{T})$ spectral tail (task complexity) nor the $\mathit{coverage}$ floor $\varepsilon_{\mathrm{cov},k}(\mathsf{A},\mathsf{L})$ that arises when essential subfunction coordinates of user k remain unobserved.

c) Annealed fundamental limits (Theorem 2): Averaging over uniformly random assignments/links under budgets (Γ, Δ) , with high probability we have:

$$B^2 \sum_{j > TN\delta} \lambda_j \quad \vee \quad \Omega(1) \cdot \mathbf{1} \{ \gamma N \delta \lesssim \log r_{\mathrm{avg}} \} \quad \leq \quad \inf_{\mathcal{D}} \overline{\mathcal{R}}(\mathcal{D}) \quad \leq \quad \tilde{\mathcal{O}} \left(\frac{B^2}{\gamma TN\delta} + \frac{\sigma^2 d_{\lambda}}{M} + B^2 \lambda + r_{\mathrm{avg}} e^{-\gamma N \delta} \right)$$

where $m_k^{\text{avg}} = TN\delta$ is the typical received-feature budget, and $r_{\text{avg}} = \frac{1}{K} \sum_{k=1}^{K} r_k$ denotes the average essential-coordinate size across users. Intuitively, r_k measures the smallest number of subfunction coordinates on which user k's target function F_k essentially depends—thus r_{avg} quantifies the overall "information footprint" or intrinsic dimensionality of the user tasks. Once $\gamma N\delta \gtrsim \log r_{\text{avg}}$, the coverage probability becomes overwhelming, making the coverage penalty negligible and ensuring that the achievable risk matches the spectral lower bound up to constant and logarithmic factors.

d) Design law and significance: Combining both regimes yields the unified scaling

Risk
$$\approx \frac{1}{\frac{\gamma N \delta T}{\sqrt{N \delta T}}} + \underbrace{\text{(kernel spectral tail)}}_{\text{task complexity}} + \underbrace{e^{-\gamma N \delta}}_{\text{coverage reliability}},$$

showing that our achievable construction attains the fundamental computation–communication–accuracy tradeoff up to constants and logarithms. Practically: increase T, N, or δ to multiply the received features $(TN\delta)$; increase γ to mitigate masking loss; ensure $\gamma N\delta \gtrsim \log r_{\rm avg}$ to eliminate coverage floors; and tune (M, λ) to control variance/bias via d_{λ} .

- e) Comparison with previous real-valued multi-user distributed computing: To compare our results with prior art—most notably Tessellated Distributed Computing (TDC) [8]—we adopt a novel kernel-theoretic and ridge-regression lens that yields an achievable scheme well beyond the linearly separable setting of TDC. Our formulation accommodates general nonlinear, smooth, and power-limited targets that encompass the vast majority of distributed learning and sensing tasks, while preserving linear decoding at the users. Crucially, in contrast to TDC's disjoint-support or cyclic-assignment structural assumptions, our GMUDC model permits arbitrary assignment and link topologies so long as they obey the computation/communication budgets (Γ, Δ) —covering heterogeneous, overlapping, and unbalanced networks—and provides both achievability and converse guarantees under these general conditions.
- f) Summary of comparison results (Section V): Specializing to the linear/isotropic regime used by [8, Thm. 2], we show that our scheme's quenched distortion is exactly the lower-tail truncated first moment of the user Gram spectrum; this enables a sharp spectral comparison to the Marchenko-Pastur (MP) benchmark:
- Match on TDC's native regime. Under disjoint-and-balanced supports (the TDC structure), the empirical Gram spectrum converges to $MP_{\lambda'}$ with $\lambda' = \Delta/\Gamma$, hence our achievable quenched distortion matches the MP envelope asymptotically. In this case our scheme is performance-equivalent to TDC.
- Quenched MP-gap. For a general (Γ, Δ) -regular topology (A, L), we define the quenched MP-gap $G^q = \Phi_{\text{MP}, \lambda'}(\kappa) D_{\text{MUDC}}^q(A, L) \geq 0$, which measures the loss relative to the MP envelope over the discarded mass $\kappa = 1 \frac{T\gamma N}{K}$. Theorem 3 gives an exact integral representation of G^q via lower-tail quantiles, proves nonnegativity, and provides a robust lower bound whenever overlaps/aliasing depress the empirical lower spectral tail.
- Tight, budget-aware upper bound. The same theorem yields a simple envelope $G^{\mathbf{q}} \leq b \left(1 \frac{T\gamma N}{K}\right)$ (e.g., $b = (1 + \sqrt{\lambda'})^2$ in the classical MP setting), showing that larger (T, γ, N) shrink the gap roughly linearly, while larger δ (for fixed γ, L, K) tightens the MP bulk and further reduces the envelope.
- Beyond tessellations. When topologies deviate from perfect tessellations (overlaps, hubs, or unbalanced links), the MP–gap is strictly positive; our framework quantifies this improvement and remains valid without structural restrictions—unlike TDC, which requires disjoint/balanced partitions.

In short, our kernel-ridge perspective strictly generalizes TDC: it recovers the MP law in TDC's regime,

extends to arbitrary budget-respecting topologies, and provides a precise spectral tool (MP-gap) to certify performance gain due to overlap or imbalance in the assignment and link topologies.

Main Contributions: This paper develops a unified learning-theoretic framework for General Multi-User Distributed Computing (GMUDC), establishing new fundamental limits for real-valued multi-user computation and learning under joint computation–communication constraints. Our main contributions are as follows:

- A unified and learning-theoretic model for multi-user real-valued distributed computation. We introduce the first general framework that models multi-user distributed computation as an inference problem in *Reproducing Kernel Hilbert Spaces (RKHSs)*. By embedding subfunction computations into kernel feature spaces and using ridge regression decoding, GMUDC bridges distributed computing, kernel approximation, and statistical learning—connecting classical distributed computation with modern learning theory.
- Novel achievable scheme with masked random Fourier features. Our achievability construction uses masked random Fourier feature (RFF) encoders that respect each server's computation budget Γ and transmit features over T shots, combined with user-wise ridge-regression decoders. This yields an unbiased Monte-Carlo kernel approximation whose variance is analytically controlled through the masking rate $\gamma = \Gamma/L$ and fan-out $\delta = \Delta/K$, enabling precise accuracy—resource scaling laws.
- First framework addressing general nonlinear functions beyond separability. Unlike all previous multi-user distributed computing formulations—limited to linearly or polynomially separable functions—GMUDC applies to all smooth, bounded-variation, or power-limited targets lying in the RKHS of any shift-invariant kernel. This includes Gaussian, Laplacian, and Matérn kernels, capturing virtually all nonlinear computations arising in distributed sensing, signal processing, and machine-learning workloads.
- Universal achievability and converse bounds valid for all topologies. We derive tight upper and lower bounds on the achievable population risk (Theorems 1–2) that hold for any assignment and link topology obeying the computation and communication budgets (Γ, Δ) . These bounds are the first to be topology-agnostic, encompassing heterogeneous, overlapping, or irregular server—user networks without assuming disjoint or cyclic structures.
- New spectral—coverage converse argument. We introduce a two-component converse combining: (i) a *spectral* limitation—characterizing the irreducible error via the eigen-tail of the kernel integral operator beyond the communicated feature budget; and (ii) a *coverage* limitation—quantifying a nonzero error floor whenever essential coordinates of a user's target function

are unobserved by the realized topology. This spectral-coverage duality establishes the first rigorous and general converse bound for real-valued multi-user distributed computation, applicable to arbitrary network topologies and subfunction assignment patterns.

- Characterization of quenched and annealed population risks. We establish two complementary risk characterizations: (i) the quenched risk, measuring instance-wise performance for a fixed topology, scaling as $\tilde{\mathcal{O}}(\frac{B^2}{\gamma m_{\text{harm}}} + \frac{\sigma^2 d_{\lambda}}{M} + B^2 \lambda)$; and (ii) the annealed risk, describing the expected performance across random topologies, scaling as $\tilde{\mathcal{O}}(\frac{B^2}{\gamma TN\delta} + e^{-\gamma N\delta})$. Together, these results reveal an explicit computation–communication–accuracy law with an exponential coverage phase transition.
- Spectral-gap analysis and topological efficiency. Through the quenched MP-gap theorem (Theorem 3), we introduce a spectral-quantile representation of the loss relative to the Marchenko-Pastur (MP) benchmark, showing that disjoint-support topologies—assumed optimal in tessellated distributed computing (TDC)—are in fact the worst-case structures in the linear regime. Topologies with partial overlaps or adaptive link reuse can achieve smaller MP-gaps, revealing new design principles for topology-efficient distributed computing.
- Bridging and generalizing Tessellated Distributed Computing. When specialized to the linear/isotropic setting of [8], our results recover TDC's Marchenko-Pastur law as a special case. However, GMUDC remains valid for arbitrary (Γ, Δ)-regular topologies, enabling analytical quantification of improvement relative to the MP envelope. Hence, our framework both extends and dominates TDC, unifying algebraic and learning-theoretic approaches.
- Applications to distributed learning and energy-efficient AI. The framework provides direct theoretical foundations for large-scale distributed and federated learning tasks—such as communication-efficient kernel regression, distributed Gaussian-process inference, and mixture-of-experts or large-language-model (LLM) architectures. By characterizing the minimal compute/communication budgets required for a target accuracy, the results support the design of energy- and data-efficient distributed AI systems operating under realistic resource constraints.
- Applications to aeronautical and aerospace systems. GMUDC naturally extends to distributed estimation and control in aeronautical and space networks, including UAV swarms, satellite constellations, and formation-flying spacecraft. The framework captures the essence of distributed Kalman filtering, consensus-based estimation, and cooperative trajectory optimization under limited inter-agent communication—enabling principled co-design of reliable, scalable, and bandwidth-aware autonomous systems.

A. Paper Organization

Section II introduces the GMUDC System Model and and formalizes the quenched and annealed risks and states the optimization problems P1 and P2. Section III presents our main theorems: Theorem 1 (quenched limits via masked RFF achievability and a spectral—coverage converse) and Theorem 2 (annealed limits under random assignments/links); Subsection III-C sketches the proofs. Section V contrasts our framework with Tessellated Distributed Computing [8], using Theorem 3 to define the MP-gap and show disjoint-support topologies are spectrally least efficient. Section VI summarizes findings and outlines extensions; appendices contain technical proofs and lemmas.

Notation: Scalars are plain (e.g., a, b, λ); vectors are bold (e.g., \mathbf{x}, \mathbf{w}); matrices use uppercase roman (e.g., G); sets are calligraphic (e.g., S, T, X). Indices: users $k \in [K] \triangleq \{1, \ldots, K\}$, servers $n \in [N]$, coordinates $\ell \in [L]$, shots $t \in [T]$, samples $i \in [M]$. For $x \in \mathcal{X} \subseteq \mathbb{R}^d$, subfunctions output are $w_{\ell} = f_{\ell}(x)$ and $\mathbf{w}(x) = (w_1, \dots, w_{\ell}) \in \mathbb{R}^L$, note that all the vectors defined in this manner are column vectors also $\mathbf{w}(x)_{-\ell}$, denotes the vectors $\mathbf{w}(x)$ with its ℓ -th coordinate removed. $K(\cdot,\cdot)$ is a positivedefinite kernel with RKHS \mathcal{H}_K and norm $\|\cdot\|_{\mathcal{H}_K}$; the associated integral operator T_K on $L^2(\mu_{\mathbf{w}})$ has nonincreasing eigenvalues $\{\lambda_j\}_{j\geq 1}$. Probability and asymptotics: $\mathbb{P}(\cdot)$ is probability, $\mathbf{1}\{\cdot\}$ is the indicator, $g \lesssim h$ means $g \leq Ch$ for an absolute constant C, and $g \approx h$ denotes two-sided \lesssim . Norms: $\|\cdot\|_2$ is Euclidean, $\|\cdot\|_{\text{op}}$ operator. All logarithms are natural unless stated otherwise. For scalars $a, b \in \mathbb{R}$ we use $a \lor b \triangleq \max\{a, b\}$ and $a \land b \triangleq \min\{a, b\}$. For $f \in \mathcal{H}_K$, the RKHS norm $||f||_{\mathcal{H}_K}$ is the Hilbert norm induced by $\langle \cdot, \cdot \rangle_{\mathcal{H}_K}$ and is characterized by the reproducing property $f(x) = \langle f, K(\cdot, x) \rangle_{\mathcal{H}_K}$ for all $x \in \mathcal{X}$. $\mathbf{1}_{\mathcal{R}} \in \{0,1\}^K$, $\mathcal{R} \subseteq [K]$ is the coordinate indicator of \mathcal{R} , $(\mathbf{1}_{\mathcal{R}})_k = 1$ if $k \in \mathcal{R}$ and 0 otherwise. Operator \odot denotes Hadamard product. $||S||_{\psi_2}$: sub-Gaussian Orlicz norm of a random variable S, defined as $||S||_{\psi_2} = \inf\{c > 0 : \mathbb{E}[\exp(S^2/c^2)] \le 2\}$, equivalently $||S||_{\psi_2} \asymp \sup_{p \ge 1} (\mathbb{E}|S|^p)^{1/p} / \sqrt{p}$. For a linear map $A: \mathbb{R}^p \to \mathbb{R}^q$, the range is Range $(A) = \{Ax: x \in \mathbb{R}^p\} \subseteq \mathbb{R}^q$. The space $L_2(\mathbb{P}_X)$ is the Hilbert space of (equivalence classes of) real-valued, square-integrable functions of the random variable X. For $f, g \in L_2(\rho)$, we also write $f \otimes g$ for the kernel $(f \otimes g)(u, v) \triangleq f(u) g(v)$, which corresponds to the operator $h \mapsto \langle h, g \rangle_{L_2(\rho)} f$. $A \succeq B$ means A - B is positive semidefinite (PSD); $A \succ B$ means A - B is positive definite (PD).

II. System Model

We consider a multi-user distributed computing system with K users, N servers, and L subfunctions. For each input sample $x \in \mathcal{X} \subseteq \mathbb{R}^d$ (with $d \in \mathbb{N}$), define

$$w_{\ell} \triangleq f_{\ell}(x), \qquad \ell \in [L],$$

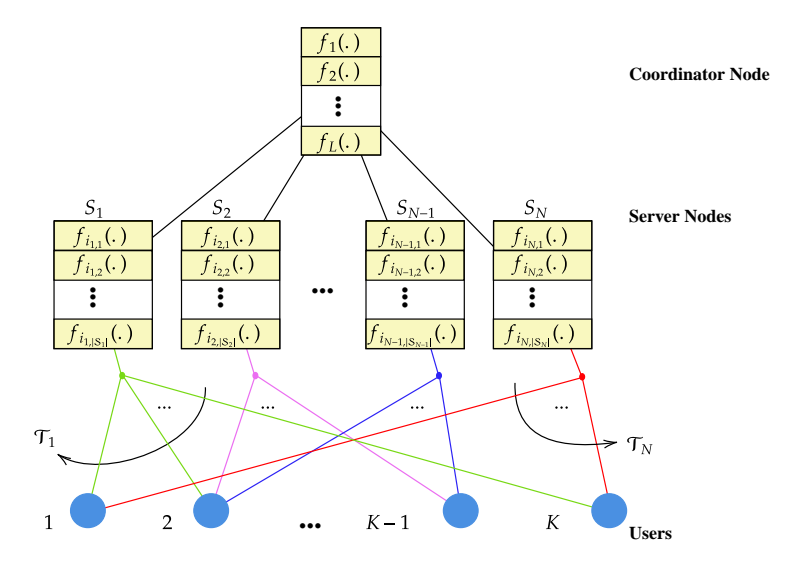


Fig. 1. The K-user, N-server, T-shot General Multi-User Distributed Computing framework considers a setting where each server n computes a subset of subfunctions $S_n = \{f_{i_{n,1}}(.), f_{i_{n,2}}(.), \dots, f_{i_{n,|S_n|}}(.)\}$ and communicates the corresponding results to a subset of users \mathcal{T}_n . This operation is performed under the computational constraint $|S_n| \leq \Gamma \leq L$ and the communication constraint $|\mathcal{T}_n| \leq \Delta \leq K$, which correspond to the normalized budgets $\gamma = \Gamma/L$ and $\delta = \Delta/K$. The system aims to minimize the population risk $\mathcal{R}(\mathcal{D} \mid A, L)$, representing the average reconstruction error of the users with respect to their desired target functions. Here, \mathcal{D} denotes the overall encoding and decoding strategy, $A = (S_1, \dots, S_N)$ specifies the computation assignments, and $L = (\mathcal{T}_1, \dots, \mathcal{T}_N)$ defines the communication topology between the servers and the users.

and collect $\mathbf{w}(x) = (w_1, \dots, w_L) \in \mathbb{R}^L$. Note that $f_{\ell}(x)$ is a subfunction to be computed by the servers. Each user $k \in [K]$ requests a target function in the RKHS of a bounded, shift-invariant kernel K, interpreted coordinate-wise:

$$F_k(x) = h_k(\mathbf{w}(x)), \quad h_k = (h_{k,1}, \dots, h_{k,m_k}), \quad h_{k,j} \in \mathcal{H}_K.$$

We assume there are no stragglers and all N servers are active in all shots. This abstraction cleanly separates the computational layer, where subfunctions f_{ℓ} are evaluated by the servers, from the task layer, where users request target functions F_k , thereby accommodating general, possibly nonlinear transformations h_k . The system operates in three sequential phases once the coordinator node receives the users' function requests. In the assignment phase, subfunctions are allocated to servers under a computation budget by the coordinator node; in the computation/encoding phase, each server computes its assigned subfunctions and applies an encoder to produce symbols to be transmitted via the error-free links in T shots to the connected users; and in the communication/decoding phase, encoded symbols are delivered to users according to the link structure, after which each user decodes

to approximate F_k . During the assignment phase, each server $n \in [N]$ is assigned a set $S_n \subseteq [L]$ of subfunctions to compute, subject to

$$|\mathcal{S}_n| \le \Gamma. \tag{1}$$

We assume each subfunction has an equally significant computational cost. In this sense, we define the normalized computation cost to be

$$\gamma \triangleq \frac{\Gamma}{L},$$

so γ represents the average replication level (fraction of subfunctions per server), governing computation–communication–risk trade-offs. We assume $1 \leq \Gamma \leq L$, hence $0 < \gamma \leq 1$.

In each of T shots, server n applies an encoder to its computed subfunctions:

$$z_{n,t}(x) = \phi_{n,t}(\{w_{\ell}(x) : \ell \in \mathcal{S}_n\}) \in \mathbb{R}, \qquad t \in [T], \qquad n \in [N].$$

The encoded symbols of server n are $\mathbf{z}_n(x) = (z_{n,1}(x), \dots, z_{n,T}(x))$. Encoders $\phi_{n,t}^{(\mathcal{S}_n)}$ may use internal randomness independent of $(\mathsf{A},\mathsf{L},\mathsf{X})$.

In the communication phase, each symbol $z_{n,t}(x)$ is made available to a subset of users through error-free links $\mathcal{T}_{n,t} \subseteq [K]$. We assume shot-agnostic links for clarity, i.e., $\mathcal{T}_{n,t} = \mathcal{T}_n$ for all $t \in [T]$. The aggregate user set served by server n obeys

$$\mathcal{T}_n \subseteq [K], \qquad |\mathcal{T}_n| \le \Delta.$$
 (3)

with normalized communication cost

$$\delta \triangleq \frac{\Delta}{K},$$

the per-server fan-out fraction (fraction of users a server can reach). We assume $1 \le \Delta \le K$, hence $0 < \delta \le 1$. User k receives the symbols

$$\mathcal{R}_k(x) = \{ z_{n,t}(x) : k \in \mathcal{T}_n \text{ and } t \in [T] \},$$
(4)

and applies a (possibly nonlinear) decoder to get an estimate of its desired function.

$$\widehat{F}_k(x) = \psi_k(\mathcal{R}_k(x)) \in \mathbb{R}^{m_k}. \tag{5}$$

A. Problem Formulation

In our annealed analysis, to expose typical-case trade-offs cleanly—without committing to a specific topology—we model assignment and links as uniformly random:

1) Random computation assignment:

$$S_n \sim \text{Unif}(\{S \subset [L] : |S| = \Gamma\})$$
 i.i.d. over n.

2) Random user links:

$$\mathcal{T}_n \sim \text{Unif}(\{U \subseteq [K] : |U| = \Delta\})$$
 i.d.d. over n .

Throughout, (A, L) are drawn independently of the data $X \sim \mathbb{P}_X$ and of any encoder randomness. This random graph model serves as an average-case benchmark, isolating the impact of (Γ, Δ, T) on performance. Note that under shot-agnostic links,

$$\underline{m}_k(\mathcal{T}) \triangleq |\mathcal{R}_k| = T |\{ n : k \in \mathcal{T}_n \} |, \tag{6}$$

where $\mathbb{E}[\underline{m}_k(\mathcal{T})] = T \frac{N\Delta}{K} = T N\delta$, which makes $N\delta$ the expected number of servers linked to any given user¹. Under the above random assignment and links (not design variables), a design only specifies the encoders and decoders as follows:

• Server encoders: for each n and $t \in [T]$ choose a measurable

$$\phi_{n,t}^{(\mathcal{S}_n)}: \mathbb{R}^{\Gamma} \to \mathbb{R}, \qquad z_{n,t}(x) = \phi_{n,t}^{(\mathcal{S}_n)}(\mathbf{w}_{\mathcal{S}_n}(x)),$$

and collect $\mathbf{z}_n(x) = (z_{n,1}(x), \dots, z_{n,T}(x)) \in \mathbb{R}^T$.

• User decoders: each user k applies

$$\psi_k: \mathbb{R}^{\underline{m}_k(\mathcal{T})} \to \mathbb{R}^{m_k}, \qquad \widehat{F}_k(x) = \psi_k(\mathcal{R}_k(x)).$$

We can see that here the encoding and decoding procedure formulation differs from [8] as it is not restricted to the set of linear functions. Now we formulate the risk (distortion) criteria.

B. Risk Criteria (Quenched vs. Annealed)

Let \mathbb{P}_X be the input distribution on \mathcal{X} , and let $A = (\mathcal{S}_1, \dots, \mathcal{S}_N)$, $L = (\mathcal{T}_1, \dots, \mathcal{T}_N)$ denote the realized assignment and links.

a) Quenched (conditional) population risk: For fixed (A, L) and a design $\mathcal{D} = (\{\phi_{n,t}^{(\cdot)}\}_{n=1,t=1}^{N,T}, \{\psi_k\}_{k=1}^K)$, define

$$\mathcal{R}(\mathcal{D} \mid \mathsf{A}, \mathsf{L}) = \mathbb{E}_{x \sim \mathbb{P}_X} \left[\frac{1}{K} \sum_{k=1}^K \left\| \psi_k(\mathcal{R}_k(x)) - h_k(\mathbf{w}(x)) \right\|_2^2 \right]. \tag{7}$$

This evaluates performance for the realized assignment/link graph.

¹Standard concentration (e.g., Hoeffding/Chernoff) implies $\underline{m}_k(\mathcal{T})$ concentrates around $TN\delta$ for each user k when N is moderate-to-large.

²Equivalently, view a single map $\phi_{n,t}: \mathbb{R}^L \times 2^{[L]} \to \mathbb{R}$ that depends only on coordinates in \mathcal{S}_n .

b) Annealed (average-over-graph) population risk: Averaging over the assignment and link randomness.

$$\overline{\mathcal{R}}(\mathcal{D}) \triangleq \mathbb{E}_{\mathsf{A},\mathsf{L}}[\mathcal{R}(\mathcal{D} \mid \mathsf{A},\mathsf{L})], \qquad (8)$$

which captures expected performance over typical random realizations.

In what follows, we precisely formulate the optimization problems that interest us:

C. Optimization Problems

P1 (Quenched design): Given (A, L), find encoders/decoders that minimize (7):

$$\begin{split} &\inf_{\mathcal{D}} \quad \mathcal{R}(\mathcal{D} \mid \mathsf{A}, \mathsf{L}) \\ &\text{s.t.} \quad \phi_{n,t}^{(\mathcal{S}_n)} : \mathbb{R}^{\Gamma} \to \mathbb{R} \text{ measurable}, \quad \psi_k : \mathbb{R}^{\underline{m}_k(\mathcal{T})} \to \mathbb{R}^{m_k} \text{ measurable}. \end{split}$$

P2 (Annealed design): The goal is to minimize the average quenched risk:

$$\inf_{\mathcal{D}} \quad \overline{\mathcal{R}}(\mathcal{D})$$
s.t. $\phi_{n,t}^{(\mathcal{S}_n)} : \mathbb{R}^{\Gamma} \to \mathbb{R}$ measurable, $\psi_k : \mathbb{R}^{\underline{m}_k(\mathcal{T})} \to \mathbb{R}^{m_k}$ measurable, (10)

In other words, P2 selects encoder/decoder families without conditioning on a specific realization of (A, L), aiming to minimize the expected (annealed) population risk over the randomness of assignments and links. Designs may depend on model parameters (e.g., Γ, Δ, T) and on \mathbb{P}_X , but not on the realized (A, L).

III. Results

In this section, we first present the encoding and decoding setups in Subsection III-A, and then state and explain the main theorems in Subsection III-B. Finally, in Subsection III-C, we provide proof sketches of the main results, including the key achievability and converse arguments as well as the resulting design takeaways.

A. Setup and Assumptions

We instantiate the encoders in (2) by masked random Fourier features (RFF) and the user decoders by ridge regression, and we benchmark against converse bounds combining an RKHS eigen-tail lower bound with a coverage floor. Let $K(\cdot, \cdot)$ be a shift-invariant kernel on \mathbb{R}^L with spectral measure μ (e.g., Gaussian RBF). Let \mathcal{H}_K denote the RKHS induced by $K(\cdot, \cdot)$, and assume each target F_k belongs to \mathcal{H}_K with $\|F_k\|_{\mathcal{H}_K} \leq B$ [44]. Training samples $\{x^{(i)}\}_{i=1}^M$, $M \in \mathbb{N}$ are i.i.d. from \mathbb{P}_X ; labels may be noisy with sub-Gaussian noise of proxy variance σ^2 . We write $\{\lambda_j\}_{j\geq 1}$ for the eigenvalues of the kernel integral operator (with respect to the pushforward of \mathbb{P}_X through \mathbf{w}), ordered nonincreasingly [45].

For each server n with assignment S_n (of size Γ) and each shot $t \in [T]$, draw independently

$$\omega_{n,t} \sim \mu, \qquad b_{n,t} \sim \text{Unif}[0, 2\pi),$$

form the masked frequency $\widetilde{\omega}_{n,t} = \omega_{n,t} \odot \mathbf{1}_{\mathcal{S}_n}, \mathbf{1}_{\mathcal{S}_n} \in \{0,1\}^L$, and emit

$$z_{n,t}(x) = \sqrt{\frac{2}{\gamma}} \cos(\widetilde{\omega}_{n,t}^{\top} \mathbf{w}(x) + b_{n,t}), \qquad \gamma \triangleq \Gamma/L.$$
 (11)

This scaling ensures (under standard masked-Bochner sampling) that $\mathbb{E}[z_{n,t}(x)z_{n,t}(x')] = K(\mathbf{w}(x), \mathbf{w}(x'))$ in expectation over (ω, b) ; more generally, it yields unbiasedness up to a masking constant absorbed by the variance proxy (cf. Lemma 1)¹.

Each user k concatenates the symbols it receives, yielding $\underline{m}_k(\mathcal{T})$ features as in (4). Given the received feature vector $\mathbf{z}_k(x) \in \mathbb{R}^{\underline{m}_k(\mathcal{T})}$, user k implements

$$\widehat{F}_{k}(x) = \beta_{k}^{\top} \mathbf{z}_{k}(x), \qquad \beta_{k} = \arg \min_{\beta \in \mathbb{R}^{\underline{m}_{k}(\mathcal{T})}} \frac{1}{M} \sum_{i=1}^{M} (\beta^{\top} \mathbf{z}_{k}(x^{(i)}) - F_{k}(x^{(i)}))^{2} + \lambda \|\beta\|_{2}^{2}.$$
 (12)

Let $d_{\lambda,k}$ denote the effective dimension of ridge at regularization λ (nonincreasing in λ , bounded by $\underline{m}_k(\mathcal{T})$).²

For user $k \in [K]$, an essential coordinate set $\mathcal{S}_k^{\star} \subseteq [L]$ for the target F_k is any set with the property that for every $\ell \in \mathcal{S}_k^{\star}$ there exist inputs $x, x' \in \mathcal{X}$ that agree on all subfunction outputs except possibly coordinate ℓ (i.e., $\mathbf{w}(x)_{-\ell} = \mathbf{w}(x')_{-\ell}$) and $||F_k(x) - F_k(x')||_2 > 0$. We define

$$r_k \triangleq \min \{ |\mathcal{S}| : \mathcal{S} \subseteq [L] \text{ is essential for } F_k \},$$

with the convention $r_k = +\infty$ if no finite essential set exists. Intuitively, r_k is the smallest number of subfunction coordinates on which F_k essentially depends. For the identity task $F_k(x) = \mathbf{w}(x)$, $r_k = L$;

¹Formally, each encoded feature can be written as $z_{n,t}(x) = \alpha M_{n,t} \varphi_{\omega,b}(\mathbf{w}(x))$, where $M_{n,t} \in \{0,1\}^{m_k}$ is a binary mask selecting the subset of features computed by server n at shot t. The mask satisfies $||M_{n,t}||_0 = \Gamma m_k$, so that only a fraction $\gamma = \Gamma$ of features is evaluated per server. Under masked Bochner sampling for a shift-invariant kernel K(u, u') = k(u - u') with $\varphi_{\omega,b}(u) = \sqrt{2}\cos(\omega^{\top}u + b)$, $b \sim \text{Unif}[0, 2\pi]$, and ω drawn from the spectral measure of k, we have $\mathbb{E}_{\omega,b}[\varphi_{\omega,b}(u)\varphi_{\omega,b}(u')] = K(u,u')$. The additional scaling $\sqrt{2/\gamma}$ compensates for the masking density, preserving the kernel expectation up to a constant factor $C_{\text{mask}} \geq 1$ that controls the induced variance.

²Let $\Phi_k(x) = (z_{n,t}(x))_{(n,t):k\in\mathcal{T}_{n,t}}$ and $G_k = \mathbb{E}[\Phi_k(x)\Phi_k(x)^{\top}] \in \mathbb{R}^{\underline{m}_k(\mathcal{T})\times\underline{m}_k(\mathcal{T})}$ be the feature covariance for user k, with eigenvalues $\{\mu_{j,k}\}$. The effective dimension at ridge parameter $\lambda > 0$ is $d_{\lambda,k} \triangleq \operatorname{tr}(G_k(G_k + \lambda I)^{-1}) = \sum_j \frac{\mu_{j,k}}{\mu_{j;k} + \lambda}$. Each summand decreases with λ , hence $d_{\lambda,k}$ is nonincreasing in λ and satisfies $0 \leq d_{\lambda,k} \leq \operatorname{rank}(G_k) \leq \underline{m}_k(\mathcal{T})$.

for a sparse linear task $F_k(x) = \sum_{\ell \in S} a_\ell w_\ell(x)$ with all $a_\ell \neq 0$, $r_k = |S|$. Here, m_{harm} denotes the harmonic mean of the per-user feature dimensions $\{m_k\}_{k=1}^K$, i.e.

$$m_{\text{harm}} = \left(\frac{1}{K} \sum_{k=1}^{K} \frac{1}{m_k}\right)^{-1}.$$

In the random assignment regime, m_{harm} is asymptotically equivalent to the arithmetic mean m_{avg} . We assume also $\gamma \geq c_0 > 0$, i.e., each server computes at least a constant fraction c_0 of subfunctions. Otherwise the bound becomes vacuous as $\gamma \to 0$.

B. Main Results

Theorem 1 describes the quenched achievability and converse for the problem P1 in (9):

Theorem 1. Fix a realization (A, L) and assume (11)–(12). There exist absolute constants $C_1, C_2, C_3 > 0$ such that, for any $\delta' \in (0,1)$ and suitable $\lambda = \lambda(M, \underline{m}_1(\mathcal{T}), \dots, \underline{m}_K(\mathcal{T}))$, the following holds with probability at least $1 - \delta'$ over the encoder randomness $\{(\omega_{n,t}, b_{n,t})\}$:

$$\mathcal{R}(\mathcal{D} \mid \mathsf{A}, \mathsf{L}) \le \left(\frac{2}{\gamma} + C_1\right) \frac{B^2}{\gamma m_{\text{harm}}} \log \frac{2}{\delta'} + C_2 \frac{\sigma^2 d_\lambda}{M} + C_3 B^2 \lambda, \tag{13}$$

where $m_{\text{harm}} \triangleq \left(\frac{1}{K}\sum_{k=1}^{K}\frac{1}{\underline{m}_{k}(\mathcal{T})}\right)^{-1}$ is the harmonic mean of the received-feature budgets, and $d_{\lambda} = 1/K\sum_{k=1}^{K}d_{\lambda,k}$, where $d_{\lambda,k} = \text{tr}(G_{k}(G_{k}+\lambda I)^{-1})$ is the effective dimension for user k. Moreover, for any encoder/decoder design that delivers $\underline{m}_{k}(\mathcal{T})$ real scalars to user k, the following quenched converse bound holds for the average risk:

$$\inf_{\mathcal{D}} \mathcal{R}(\mathcal{D} \mid \mathsf{A}, \mathsf{L}) \geq \frac{B^2}{K} \sum_{k=1}^{K} \Big(\sum_{j > m_k(\mathcal{T})} \lambda_j \vee \varepsilon_{\mathrm{cov}, k}(\mathsf{A}, \mathsf{L}) \Big), \tag{14}$$

where $(\lambda_j)_{j\geq 1}$ are the eigenvalues of the kernel integral operator (in nonincreasing order), and $\varepsilon_{cov,k}(A,L) > 0$ whenever, for the realized (A,L), the set of server assignments fails to cover the essential coordinate set of user k's target.

Remark 1. The normalized computation cost $\gamma = \Gamma/L$ captures the masking penalty (each feature "sees" a fraction γ of coordinates of $\mathbf{w}(x)$). The achievability bound (13) improves with more received features $\underline{m}_k(\mathcal{T}) = T|\{n: k \in \mathcal{T}_n\}|$, larger compute fraction γ , more samples M, and proper λ . The converse (14) matches the best \underline{m}_k -rank kernel approximation and enforces a nonzero floor if coverage fails in the realized graph. Note that in the quenched setting the normalized communication budget δ does not appear explicitly; its effect is entirely mediated through the realized feature count $\underline{m}_k(\mathcal{T})$ and the coverage event. By contrast, in the annealed regime δ re-emerges in the expectation $\mathbb{E}[\underline{m}_k(\mathcal{T})] = TN\delta$ and in the exponential coverage term.

The next result gives annealed upper and lower bounds for P2 in (10).

Theorem 2. Under the assumptions of Theorem 1, and after averaging over the random computation assignments A and link patterns L, the optimal annealed population risk satisfies

$$B^{2} \sum_{j > m_{k}^{\text{avg}}} \lambda_{j} \vee c' \mathbf{1} \{ \gamma N \delta \lesssim \log(r_{\text{avg}}) \} \leq \inf_{\mathcal{D}} \overline{\mathcal{R}}(\mathcal{D}) \leq \mathsf{U}_{\text{ann}}, \tag{15}$$

with

$$\mathsf{U}_{\mathrm{ann}} \leq \left(\frac{2}{\gamma} + C_1\right) \frac{B^2}{\gamma T (1-\varepsilon) N \delta} + C_2 \frac{\sigma^2 d_{\lambda}}{M} + C_3 B^2 \lambda + r_{\mathrm{avg}} e^{-\gamma N \delta} + \exp(-c \varepsilon^2 N \delta) C_{\star}, (16)$$

where $m_k^{\text{avg}} \triangleq TN\delta$, and $r_{\text{avg}} \triangleq \frac{1}{K} \sum_{k=1}^K r_k$, and $\epsilon \in (0,1)$ is a small positive deviation parameter. Here, $\gamma = \Gamma/L$ and $\delta = \Delta/K$ are the normalized computation and communication costs; $\{\lambda_j\}_{j\geq 1}$ are the nonincreasing eigenvalues of the kernel integral operator associated with K under the law of $\mathbf{w}(X)$; r_k is the size of an essential coordinate set for F_k ; and $C_1, C_2, C_3, c, c', C_{\star} > 0$ are absolute constants independent of $(N, K, L, \Gamma, \Delta, T, M)$.

Remark 2. In the annealed regime, $\underline{m}_k(\mathcal{T})$ concentrates around $m_k^{\text{avg}} = TN\delta$, so the achievability bound behaves like $(2/\gamma + C_1)B^2/(\gamma m_k^{\text{avg}})$ up to logarithmic factors, while the eigen-tail converse uses the same feature budget. The small additive term $r_{\text{avg}} e^{-c\gamma N\delta}$ accounts for the (averaged) exponentially small chance of a coverage miss. Hence, once $\gamma N\delta$ exceeds the (logarithmic) coverage threshold in $\log r_{\text{avg}}$, the scheme is order-optimal up to constants.

C. Proof Sketches of Theorems 1 and 2

The proof of Theorem 1 (quenched bounds) and Theorem 2 (annealed bounds) follows from two complementary arguments: an achievability construction based on masked random-feature encoders and a converse argument based on spectral and coverage limitations. Both parts rely on the spectral structure of the user-dependent Gram matrices and the effective feature dimensions induced by the computation and communication budgets.

For Theorem 1, the achievability argument fixes the topology (A, L) and shows that the proposed masked random-feature encoder, combined with the ridge decoder, attains the upper bound in (13). Each server uses a mask of size Γ and emits features $z_{n,t}(x) = \sqrt{2/\gamma} \cos((\omega_{n,t} \odot 1_{S_n})^{\top} w(x) + b_{n,t})$ with $\gamma = \Gamma/L$. This yields an unbiased Monte Carlo approximation of the target kernel for each user once the $m_k(\mathcal{T}) = T|\{n : k \in \mathcal{T}_n\}|$ received scalars are concatenated. A Bernstein-style concentration argument with masking variance control gives a kernel approximation error of order $(2/\gamma^2 m_k(\mathcal{T}) + C'/(\gamma m_k(\mathcal{T}))) \log(2/\delta')$. Substituting this into the standard kernel ridge decomposition

yields the prediction risk bound $\mathcal{R}(\mathcal{D} \mid \mathsf{A}, \mathsf{L}) \lesssim (C_1 + 1/\gamma)B^2/(\gamma m_k(\mathcal{T})) + \sigma^2 d_{\lambda}/M + B^2 \lambda$, where $d_{\lambda} = 1/K \sum_{k=1}^{K} d_{\lambda,k}, d_{\lambda,k} = \operatorname{tr}(G_k(G_k + \lambda I)^{-1})$ is the ridge effective dimension. Averaging over users introduces the harmonic mean m_{harm} and gives the quenched achievability inequality (13).

The converse of Theorem 1 combines a spectral tail limitation with a coverage floor. Any scheme that communicates at most $m_k(\mathcal{T})$ scalars per user confines the reconstruction to an $m_k(\mathcal{T})$ -dimensional subspace of $L_2(\mathbb{P}_X)$. By the theory of Kolmogorov m-widths for RKHS balls, the minimum achievable risk equals the energy of the discarded spectral tail $B^2 \sum_{j>m_k(T)} \lambda_j$. If an essential coordinate of user k is never computed and transmitted in the realized topology, then inputs differing only on that coordinate are indistinguishable, producing a coverage floor $\varepsilon_{\text{cov},k}(A,L) > 0$. Combining both limitations yields the quenched converse bound (14).

Theorem 2 concerns the annealed regime, obtained by averaging over the random assignment and link topologies. For the achievability part, the number of features received by each user satisfies $|\{n:k\in\mathcal{T}_n\}|\sim \text{Binomial}(N,\delta)$, so $m_k(\mathcal{T})$ concentrates around $m_k^{\text{avg}}=TN\delta$. Substituting m_k^{avg} into the quenched bound and accounting for the exponentially small deviation probability $\exp(-c\varepsilon^2N\delta)$ gives the annealed upper bound U_{ann} in (16). The additional coverage term $r_{\text{avg}}\exp(-\gamma N\delta)$ captures the small probability of missing an essential coordinate across users. Collecting all constants and averaging over (A, L) yields the complete achievability part of Theorem 2.

The converse in the annealed regime follows by averaging the spectral tail bound over (A, L). Taking the expectation and using the convexity of $m \mapsto \sum_{j>m} \lambda_j$ gives $\inf_{\mathcal{D}} \overline{\mathcal{R}}(\mathcal{D}) \geq B^2 \sum_{j>m} \lambda_j$, with $m_k^{\text{avg}} = TN\delta$. When $\gamma N\delta$ is below the logarithmic threshold $\log(r_{\text{avg}})$, coverage failures occur with nonnegligible probability and impose a constant risk floor, represented by the term $c'\mathbf{1}\{\gamma N\delta \lesssim \log(r_{\text{avg}})\}$. Combining these elements establishes the annealed lower bound and completes the proof of Theorem 2.

IV. Proof of Theorem 1 and Theorem 2

We prove Theorem 1 in Subsection IV-A and Theorem 2 in Subsection IV-B.

A. Proof of Theorem 1

We prove the achievability and converse bounds in two parts. Throughout, (A, L) is fixed (quenched), and the only randomness is from the encoder draws $\{(\omega_{n,t}, b_{n,t})\}$ as specified in (11). For user k, let $\underline{m}_k \triangleq \underline{m}_k(\mathcal{T})$ denote the number of received scalars (features). Stack them into a feature map

$$\Phi_k(x) \in \mathbb{R}^{\underline{m}_k}, \qquad \Phi_k(x) = (z_{n,t}(x))_{(n,t):k \in \mathcal{T}_{n,t}}.$$

Define the (population) feature covariance and the effective ridge dimension

$$G_k \triangleq \mathbb{E}_x \left[\Phi_k(x) \Phi_k(x)^\top \right] \in \mathbb{R}^{\underline{m}_k \times \underline{m}_k}, \qquad d_{\lambda,k} = \operatorname{tr} \left(G_k(G_k + \lambda I)^{-1} \right) \in (0, \underline{m}_k]. \tag{17}$$

We assume the standard kernel setup from the theorem statement: $F_k \in \mathcal{H}_K$ with $||F_k||_{\mathcal{H}_K} \leq B$, where K(.,.) is a shift-invariant kernel on \mathbb{R}^L with eigenvalues $\{\lambda_j\}_{j\geq 1}$ (nonincreasing) with respect to the distribution of $\mathbf{w}(x)$. Because each feature is computed from a masked vector $(\omega_{n,t} \odot \mathbf{1}_{\mathcal{S}_n})$, we isolate the impact of masking via a single constant $C_{\text{mask}} \geq 1$. In particular, we have:

Lemma 1. Let $K(u,v) = \kappa(u-v)$ be a shift-invariant kernel on \mathbb{R}^L with Bochner spectral measure [44] μ satisfying $\int \|\omega\|_2^2 d\mu(\omega) < \infty$ and $|K(u,v)| \leq 1$. Fix a subset $S \subseteq [L]$ with $|S| = \Gamma$ and let $\gamma = \Gamma/L$. Define the masked RFF

$$\phi(x; \omega, b, \mathcal{S}) = \sqrt{\frac{2}{\gamma}} \cos((\omega \odot \mathbf{1}_{\mathcal{S}})^{\mathsf{T}} \mathbf{w}(x) + b), \qquad \omega \sim \mu, \quad b \sim \mathrm{Unif}[0, 2\pi].$$

Assume $\|\mathbf{w}(x)\|_2 \leq R$ almost surely (or, more generally, $\mathbf{w}(x)$ is sub-Gaussian with parameter depending only on R). Then there exists an absolute constant $C_{\text{mask}} \geq 1$ (depending only on K and R, but not on x, x', L, Γ) and a bounded variance proxy $V_K(u, v) \leq 1$ for the unmasked RFF estimator, where

$$V_K(u,v) \triangleq \|K(\cdot,u) - K(\cdot,v)\|_{\mathcal{H}_K}^2 = K(u,u) + K(v,v) - 2K(u,v), \tag{18}$$

such that, for all x, x' with $u = \mathbf{w}(x)$ and $v = \mathbf{w}(x')$,

$$\operatorname{Var}[\phi(x;\omega,b,\mathcal{S})\,\phi(x';\omega,b,\mathcal{S})] \leq \frac{1}{2\gamma^2} + \frac{C_{\text{mask}}}{\gamma} \,V_K(u,v). \tag{19}$$

Moreover, if the masked frequency is sampled from the masked Bochner law (i.e., draw $\omega_{\mathcal{S}} \sim \mu$ on \mathbb{R}^{Γ} and embed as $\widetilde{\omega} = (\omega_{\mathcal{S}}, 0_{\mathcal{S}^c})$), then (19) holds with $C_{\text{mask}} = 1$.

The proof of Lemma 1 is provided in Appendix A. Note that in the proof we assume that the random frequencies $\{(\omega_{n,t},b_{n,t})\}$ used by different servers and shots are drawn independently across (n,t) and independently of the masking pattern (A,L). Hence conditional on (A,L), the masked feature vectors are independent across servers. This ensures that concentration inequalities for Monte-Carlo kernel estimates apply.

1) Achievability of Theorem 1: The proof proceeds through three main steps: (i) establishing a concentration bound for the kernel approximation using masked random Fourier features (Lemma 2); (ii) deriving a general excess-risk decomposition for ridge regression with random features (Lemma 3); and (iii) combining these results to obtain a uniform high-probability bound averaged over users.

Lemma 2. Let $\widetilde{K}_k(x, x') \triangleq \frac{1}{m_k} \Phi_k(x)^{\top} \Phi_k(x')$ be the Monte Carlo kernel built from the m_k masked-RFF features received by user k. Then, for any $\delta' \in (0, 1)$, with probability at least $1 - \delta'$ over the encoder randomness,

$$\mathbb{E}_{x,x'}\left[\left(\widetilde{K}_k(x,x') - K(\mathbf{w}(x),\mathbf{w}(x'))\right)^2\right] \leq \left(\frac{2}{\gamma^2 m_k} + \frac{C_1'}{\gamma m_k}\right) \log \frac{2}{\delta'},\tag{20}$$

for an absolute constant $C'_1 > 0$ depending only on the kernel family (via V_K) and C_{mask} in Lemma 1.

The proof of Lemma 2 is provided in Appendix B. Lemma 2 establishes that the masked-RFF approximation of the kernel K converges in mean square at rate $1/(\gamma m_k)$, up to logarithmic factors, where $\gamma = \Gamma/L$ captures the fraction of coordinates each encoder observes. Building on this approximation result, the next lemma provides a general bound on the prediction risk of the ridge estimator in terms of its bias and variance components, under an arbitrary feature map Φ_k .

Lemma 3. Let \widehat{F}_k be the ridge predictor (12) trained with M samples and feature map Φ_k . Then, for any $\lambda > 0$,

$$\mathbb{E}_{x}[\|\widehat{F}_{k}(x) - F_{k}(x)\|_{2}^{2}] \leq \inf_{\beta \in \mathbb{R}^{m_{k}}} \mathbb{E}_{x}[(\beta^{\top} \Phi_{k}(x) - F_{k}(x))^{2}] + C_{2}' \frac{\sigma^{2} d_{\lambda,k}}{M} + C_{3}' B^{2} \lambda, \quad (21)$$

where $d_{\lambda,k}$ is given in (17), and $C'_2, C'_3 > 0$ are absolute constants.

The proof of Lemma 3 is provided in Appendix C. Before proceeding, we recall that the masked Random Fourier Feature approximation affects the ridge bias through the kernel operator perturbation. Following the standard analysis of kernel ridge regression (see, e.g., [46]), if \hat{G} denotes the empirical (masked) kernel matrix and $\|\hat{G} - G\|_{op} \leq \varepsilon_{RFF}$, then

$$\|(\widehat{G} + \lambda I)^{-1}g - (G + \lambda I)^{-1}g\| = O\left(\frac{\varepsilon_{\text{RFF}}}{\lambda}\right),$$

which implies that the ridge estimator inherits an additive bias term of order $O(\varepsilon_{RFF}/\lambda)$. Hence, the population risk bound of Lemma 3 remains valid up to this small correction, justifying the substitution of the masked kernel approximation into the subsequent risk decomposition

Combining Lemmas 2 and 3: from kernel error to prediction risk

We now make precise why, when $F_k \in \mathcal{H}_K$ with $||F_k||_{\mathcal{H}_K} \leq B$, the best linear predictor in the masked-RFF feature space has approximation error controlled by the $L_2(\mathbb{P}_X)$ kernel mismatch between K and \widetilde{K}_k . Let ρ be the distribution of $U = \mathbf{w}(X) \in \mathbb{R}^L$ induced by $X \sim \mathbb{P}_X$. For a (symmetric, PSD) kernel $Q : \mathbb{R}^L \times \mathbb{R}^L \to \mathbb{R}$, define the integral operator

$$(T_Q f)(u) = \int Q(u, v) f(v) d\rho(v), \qquad f \in L_2(\rho).$$

We write T_K and $T_{\widetilde{K}_k}$ for the operators with kernels K and \widetilde{K}_k , respectively. Their Hilbert–Schmidt (HS) norms satisfy

$$||T_K - T_{\widetilde{K}_k}||_{HS}^2 = \iint (K(u, v) - \widetilde{K}_k(u, v))^2 d\rho(u) d\rho(v)$$
 (22)

$$= \mathbb{E}_{x,x'} \left[\left(K(\mathbf{w}(x), \mathbf{w}(x')) - \widetilde{K}_k(x, x') \right)^2 \right]. \tag{23}$$

Let \mathcal{H}_K be the RKHS of K. The canonical inclusion $\mathcal{H}_K \hookrightarrow L_2(\rho)$ is continuous and satisfies the isometry identity

$$\langle f, g \rangle_{\mathcal{H}_K} = \langle T_K^{-1/2} f, T_K^{-1/2} g \rangle_{L_2(\rho)} \quad \text{for all } f, g \in \mathcal{H}_K.$$
 (24)

In particular, $||f||_{\mathcal{H}_K}^2 = ||T_K^{-1/2}f||_{L_2(\rho)}^2$ and $f(u) = \langle f, K(u, \cdot) \rangle_{\mathcal{H}_K}$.

The (masked-RFF) feature map collected at user k induces an approximate kernel

$$\widetilde{K}_k(u,v) = \frac{1}{m_k} \Phi_k(u)^{\top} \Phi_k(v),$$

which is PSD. Its RKHS $\mathcal{H}_{\widetilde{K}_k}$ equals the closure of the linear span of $\{\widetilde{K}_k(\cdot,v):v\in\mathbb{R}^L\}$ with inner product determined by \widetilde{K}_k . Every linear predictor in the feature space is a function $g\in\mathcal{H}_{\widetilde{K}_k}$ of the form

$$g(u) = \beta^{\top} \Phi_k(u) \iff g(\cdot) \in \mathcal{H}_{\widetilde{K}_k}, \quad \|g\|_{\mathcal{H}_{\widetilde{K}_k}} = \|\beta\|_2.$$

Hence

$$\inf_{\beta \in \mathbb{R}^{m_k}} \mathbb{E}[(\beta^{\top} \Phi_k(X) - F_k(X))^2] = \inf_{g \in \mathcal{H}_{\widetilde{K}_k}} \|g - F_k\|_{L_2(\rho)}^2.$$
 (25)

Let $P_{\widetilde{K}_k}: L_2(\rho) \to \overline{\mathcal{H}_{\widetilde{K}_k}}$ be the $L_2(\rho)$ -orthogonal projection onto the closure of $\mathcal{H}_{\widetilde{K}_k}$ in $L_2(\rho)$. Then the optimal $g^* = P_{\widetilde{K}_k} F_k$ and the approximation error is

$$\inf_{g \in \mathcal{H}_{\widetilde{K}}} \|g - F_k\|_{L_2(\rho)}^2 = \|(I - P_{\widetilde{K}_k})F_k\|_{L_2(\rho)}^2.$$

A standard comparison yields, for all $f \in \mathcal{H}_K^{-1}$,

Hilbert-Schmidt operators. This is the claimed comparison bound.

$$\|(I - P_{\widetilde{K}_{L}})f\|_{L_{2}(\rho)}^{2} \le \|f\|_{\mathcal{H}_{K}}^{2} \|T_{K} - T_{\widetilde{K}_{L}}\|_{HS}.$$
 (26)

Let $\{(\lambda_j, \varphi_j)\}_{j\geq 1}$ be the Mercer eigen-system of T_K on $L_2(\rho)$. Any $f \in \mathcal{H}_K$ can be written as $f = \sum_j a_j \varphi_j$ with $\sum_j a_j^2 / \lambda_j < \infty$ and $||f||_{\mathcal{H}_K}^2 = \sum_j a_j^2 / \lambda_j$. Let $T_\Delta = T_K - T_{\widetilde{K}_k}$. Then, by orthogonality and Cauchy-Schwarz in the HS inner product,

$$\|(I - P_{\widetilde{K}_k})f\|_{L_2(\rho)}^2 = \sup_{\|h\|_{L_2} \le 1} \left\langle (I - P_{\widetilde{K}_k})f, h \right\rangle_{L_2}^2 \le \left\langle f, T_{\Delta}f \right\rangle_{L_2} \le \|f\|_{\mathcal{H}_K}^2 \|T_{\Delta}\|_{HS},$$

One convenient derivation works directly in $L_2(\rho)$. Let $V \equiv \overline{\mathcal{H}_{\widetilde{K}_k}}$ and $P \equiv P_{\widetilde{K}_k}$ be the $L_2(\rho)$ -orthogonal projector onto V. For any $f \in \mathcal{H}_K$, one has $\|(I-P)f\|_{L_2}^2 = \sup_{\|h\|_{L_2} \leq 1, \ h \perp V} \langle (I-P)f, h \rangle_{L_2}^2 = \sup_{\|h\|_{L_2} \leq 1, \ h \perp V} \langle f, h \rangle_{L_2}^2$. Write T_K and $T_{\widetilde{K}}$ for the Mercer operators of K and \widetilde{K} , and use the RKHS isometry $\langle f, g \rangle_{\mathcal{H}_K} = \langle T_K^{-1/2}f, T_K^{-1/2}g \rangle_{L_2}$. Then $\langle f, h \rangle_{L_2} = \langle T_K^{-1/2}f, T_K^{1/2}h \rangle_{L_2} \leq \|f\|_{\mathcal{H}_K}$ $\|T_K^{1/2}h\|_{L_2}$. If $h \perp V = \overline{\mathrm{Range}(J_{\widetilde{K}})}$, then $J_{\widetilde{K}}^*h = 0$, hence $\langle h, T_{\widetilde{K}}h \rangle = \|J_{\widetilde{K}}^*h\|_{\mathcal{H}_{\widetilde{K}}}^2 = 0$ and therefore $\|T_K^{1/2}h\|_{L_2}^2 = \langle h, T_K h \rangle = \langle h, (T_K - T_{\widetilde{K}})h \rangle \leq \|T_K - T_{\widetilde{K}}\|_{\mathrm{op}} \|h\|_{L_2}^2$. Combining these and taking the supremum over such h gives

 $\|(I-P)f\|_{L_2}^2 \leq \|f\|_{\mathcal{H}_K}^2 \|T_K - T_{\widetilde{K}}\|_{\text{op}} \leq \|f\|_{\mathcal{H}_K}^2 \|T_K - T_{\widetilde{K}}\|_{\text{HS}}, \text{ where the last inequality uses } \|\cdot\|_{\text{op}} \leq \|\cdot\|_{\text{HS}} \text{ for } \|T_K - T_{\widetilde{K}}\|_{\text{HS}}, \text{ where the last inequality uses } \|\cdot\|_{\text{op}} \leq \|\cdot\|_{\text{HS}} \|T_K - T_{\widetilde{K}}\|_{\text{HS}}, \text{ where the last inequality uses } \|\cdot\|_{\text{op}} \leq \|\cdot\|_{\text{HS}} \|T_K - T_{\widetilde{K}}\|_{\text{HS}}, \text{ where the last inequality uses } \|\cdot\|_{\text{op}} \leq \|f\|_{\text{HS}}^2 \|T_K - T_{\widetilde{K}}\|_{\text{HS}}, \text{ where the last inequality uses } \|\cdot\|_{\text{op}} \leq \|f\|_{\text{HS}}^2 \|T_K - T_{\widetilde{K}}\|_{\text{HS}}, \text{ where the last inequality uses } \|\cdot\|_{\text{op}} \leq \|f\|_{\text{HS}}^2 \|T_K - T_{\widetilde{K}}\|_{\text{HS}}, \text{ where the last inequality uses } \|\cdot\|_{\text{op}} \leq \|f\|_{\text{HS}}^2 \|T_K - T_{\widetilde{K}}\|_{\text{HS}}, \text{ where the last inequality uses } \|\cdot\|_{\text{op}} \leq \|f\|_{\text{HS}}^2 \|T_K - T_{\widetilde{K}}\|_{\text{HS}}, \text{ where the last inequality uses } \|\cdot\|_{\text{op}} \leq \|f\|_{\text{HS}}^2 \|T_K - T_{\widetilde{K}}\|_{\text{HS}}, \text{ where } \|f\|_{\text{HS}}^2 \|T_K - T_{\widetilde{K}}\|_{\text{HS}}$

where in the last step we used the isometry (24) by writing $f = T_K^{1/2}h$ with $||h||_{L_2} = ||f||_{\mathcal{H}_K}$ and bounding $\langle f, T_{\Delta} f \rangle = \langle h, T_K^{1/2} T_{\Delta} T_K^{1/2} h \rangle \leq ||T_K||_{\text{op}} ||T_{\Delta}||_{\text{HS}} ||h||_{L_2}^2$. A rigorous proof can be given by truncating the Mercer expansion and passing to the limit; we omit further details for brevity.¹

Combining (25) and (26) with $f = F_k$ and $||F_k||_{\mathcal{H}_K} \leq B$,

$$\inf_{\beta} \mathbb{E}[(\beta^{\top} \Phi_k(X) - F_k(X))^2] = \inf_{g \in \mathcal{H}_{\widetilde{K}_k}} \|g - F_k\|_{L_2(\rho)}^2 \le B^2 \|T_K - T_{\widetilde{K}_k}\|_{HS}.$$
 (27)

Using (22) and the identity for HS norm,

$$||T_K - T_{\widetilde{K}_k}||_{HS} = \left(\mathbb{E}_{x,x'}[(K(\mathbf{w}(x), \mathbf{w}(x')) - \widetilde{K}_k(x, x'))^2]\right)^{1/2}.$$
 (28)

Squaring both sides of (27) and (28) gives the central inequality:

$$\inf_{\beta} \mathbb{E}[(\beta^{\top} \Phi_k(X) - F_k(X))^2] \leq B^2 \cdot \mathbb{E}_{x,x'}[(\widetilde{K}_k(x,x') - K(\mathbf{w}(x), \mathbf{w}(x')))^2]. \tag{29}$$

By Lemma 2, with probability at least $1 - \delta'$ over encoder draws,

$$\mathbb{E}_{x,x'}[(\widetilde{K}_k(x,x') - K(\mathbf{w}(x),\mathbf{w}(x')))^2] \leq \left(\frac{2}{\gamma} + C_1'\right) \frac{1}{\gamma m_k} \log \frac{2}{\delta'}.$$

Plugging this into (29),

$$\inf_{\beta} \mathbb{E}[(\beta^{\top} \Phi_k(X) - F_k(X))^2] \leq \left(\frac{2}{\gamma} + C_1'\right) \frac{B^2}{\gamma m_k} \log \frac{2}{\delta'}.$$

Finally, substituting this bound into Lemma 3 yields, for the same event.

$$\mathbb{E}_{X}[\|\widehat{F}_{k}(X) - F_{k}(X)\|_{2}^{2}] \leq \left(\frac{2}{\gamma} + C_{1}'\right) \frac{B^{2}}{\gamma m_{k}} \log \frac{2}{\delta'} + C_{2}' \frac{\sigma^{2} d_{\lambda,k}}{M} + C_{3}' B^{2} \lambda.$$

Averaging this inequality over all $k \in [K]$, we obtain²

$$\frac{1}{K} \sum_{k=1}^K \mathbb{E}_X \big[\| \widehat{F}_k(X) - F_k(X) \|_2^2 \big] \leq \left(\frac{2}{\gamma} + C_1' \right) \frac{B^2}{\gamma} \left(\frac{1}{K} \sum_{k=1}^K \frac{1}{m_k} \right) \log \frac{2}{\delta'} + C_2' \frac{\sigma^2 d_\lambda}{M} + C_3' B^2 \lambda.$$

Recalling the definition of the quenched risk

$$\mathcal{R}(\mathcal{D} \mid \mathsf{A}, \mathsf{L}) = \mathbb{E}_X \left[\frac{1}{K} \sum_{k=1}^K \|\widehat{F}_k(X) - F_k(X)\|_2^2 \right],$$

¹For a rigorous justification of the step $\langle f, T_{\Delta} f \rangle \leq \|f\|_{\mathcal{H}_K}^2 \|T_{\Delta}\|_{\mathrm{HS}}$, expand $f \in \mathcal{H}_K$ in the Mercer eigenbasis of T_K . Write $f = \sum_{j=1}^{\infty} a_j \varphi_j$ where $\{\varphi_j\}$ are the eigenfunctions of T_K with eigenvalues $\{\lambda_j\}$, so that $\|f\|_{\mathcal{H}_K}^2 = \sum_j a_j^2 / \lambda_j$ and $\|f\|_{L_2(\rho)}^2 = \sum_j a_j^2$. Then $\langle f, T_{\Delta} f \rangle = \sum_{i,j} a_i a_j \langle \varphi_i, T_{\Delta} \varphi_j \rangle$. By Cauchy–Schwarz in the Hilbert–Schmidt inner product, $|\langle f, T_{\Delta} f \rangle| \leq \|f \otimes f\|_{\mathrm{HS}} \|T_{\Delta}\|_{\mathrm{HS}}$. But $\|f \otimes f\|_{\mathrm{HS}} = \|f\|_{L_2}^2 = \sum_j a_j^2 \leq \|f\|_{\mathcal{H}_K}^2 \max_j \lambda_j \leq \|T_K\|_{\mathrm{op}} \|f\|_{\mathcal{H}_K}^2$. Hence $|\langle f, T_{\Delta} f \rangle| \leq \|T_K\|_{\mathrm{op}} \|f\|_{\mathcal{H}_K}^2 \|T_{\Delta}\|_{\mathrm{HS}}$, which is the claimed bound. A more careful argument can be given by truncating the Mercer series and then passing to the limit, but the inequality follows directly from Hilbert–Schmidt duality.

²Averaging the per-user risks yields the harmonic mean since each individual term scales inversely with the available feature count m_k . This follows from Jensen's inequality applied to the convex function $x \mapsto 1/x$, ensuring that the averaged risk over heterogeneous users depends on m_{harm} rather than the arithmetic mean m_{avg} .

and denoting by

$$m_{\text{harm}} \triangleq \left(\frac{1}{K} \sum_{k=1}^{K} \frac{1}{m_k}\right)^{-1}$$

the harmonic mean of the user budgets, we conclude that on the same event

$$\mathcal{R}(\mathcal{D} \mid \mathsf{A}, \mathsf{L}) \; \leq \; \left(\frac{2}{\gamma} + C_1'\right) \, \frac{B^2}{\gamma \, m_{\mathrm{harm}}} \, \log \frac{2}{\delta'} \; + \; C_2' \, \frac{\sigma^2 d_\lambda}{M} \; + \; C_3' \, B^2 \lambda,$$

which is exactly the bound $(13)^1$.

2) Converse of Theorem 1: We prove the two terms in (14) separately.

Lemma 4. Fix $m \in \mathbb{N}$. For any measurable scheme (encoders/decoders) that delivers at most m real scalars to user k per input, we have

$$\inf_{schemes\ with\ \leq\ m\ scalars} \mathbb{E}_x\big[\|\widehat{F}_k(x) - F_k(x)\|_2^2\big] \ \geq\ B^2 \sum_{j>m} \lambda_j.$$

The proof of Lemma 4 is provided in Appendix D. Applying Lemma 4 with $m = m_k(\mathcal{T})$ gives the eigen-tail term in (14).

Lemma 5. Suppose there exists a coordinate set $S_k^* \subseteq [L]$ on which F_k essentially depends, and that for the realized (A, L) there exists $\ell^* \in S_k^*$ such that $\{n : \ell^* \in S_n, k \in \mathcal{T}_n\} = \emptyset$. Then there exists a constant $\varepsilon_{\text{cov},k}(A, L) > 0$ such that for any scheme,

$$\mathbb{E}_x [\|\widehat{F}_k(x) - F_k(x)\|_2^2] \geq \varepsilon_{\text{cov},k}(\mathsf{A},\mathsf{L}).$$

The proof of Lemma 5 is provided in Appendix E. By Lemma 4 and Lemma 5, for any design that delivers $m_k(\mathcal{T})$ real scalars to user k, we have the per-user lower bound

$$\mathbb{E}_{X}[\|\widehat{F}_{k}(X) - F_{k}(X)\|_{2}^{2}] \geq B^{2} \sum_{j>m_{k}(\mathcal{T})} \lambda_{j} \vee \varepsilon_{\text{cov},k}, \tag{30}$$

Averaging (30) over $k \in [K]$ yields the quenched average-risk lower bound as stated in Theorem 1.

¹Strictly speaking, the concentration lemma can be stated either (i) uniformly over all $k \in [K]$, in which case the above bound holds on a single high-probability event without any union bound, or (ii) per-user, in which case one may either absorb the log K factor into the constants by a union bound, or argue directly on the average risk using Bernstein's inequality. In both cases the resulting rate remains unchanged, and the bound in Theorem 1 follows.

B. Proof of Theorem 2

We prove the annealed *upper* and *lower* bounds separately. Throughout, we use the assumptions of Theorem 1 and average over the random computation assignments A and link patterns L (both independent of the data and of the encoder randomness). For a fixed user k, recall

$$\underline{m}_k = \underline{m}_k(\mathcal{T}) = T |\{ n \in [N] : k \in \mathcal{T}_n \}|, \qquad \underline{m}_k^{\text{avg}} = \mathbb{E}_{\mathsf{A},\mathsf{L}}[\underline{m}_k(\mathcal{T})] = T \, N \, \delta, \qquad r_{\text{avg}} = \frac{1}{K} \sum_{k=1}^K r_k.$$

In the quenched analysis (Theorem 1), \underline{m}_k is treated as a deterministic quantity determined by a fixed topology (A, L). In contrast, in the annealed setting of Theorem 2, \underline{m}_k becomes a random variable through the random link assignments L and computation patterns A. Hence, expectations such as $\mathbb{E}_{A,L}[\underline{m}_k]$ or $\mathbb{E}_{A,L}[1/\underline{m}_k]$ are taken over these random topologies, while the quenched risk $\mathcal{R}(\mathcal{D} \mid A, L)$ conditions on a fixed realization. This distinction ensures consistency between the two analyses.

a) Part I (Achievability): Fix a realization (A, L). By Theorem 1, with probability at least $1 - \delta_0$ over the encoder draws,

$$\mathcal{R}(\mathcal{D} \mid \mathsf{A}, \mathsf{L}) \leq \left(\frac{2}{\gamma} + C_1\right) \frac{B^2}{\gamma} \left(\frac{1}{K} \sum_{k=1}^K \frac{1}{m_k}\right) \log \frac{2}{\delta_0} + C_2 \frac{\sigma^2 d_\lambda}{M} + C_3 B^2 \lambda. \tag{31}$$

For each k, let

$$\operatorname{Bad}_k(\varepsilon) \triangleq \left\{ \left| \left\{ n : k \in \mathcal{T}_n \right\} \right| < (1 - \varepsilon) N \delta \right\}, \quad 0 < \varepsilon < 1.$$

Since $|\{n: k \in \mathcal{T}_n\}| \sim \text{Binomial}(N, \delta)$, Chernoff's bound gives

$$\Pr(\operatorname{Bad}_k(\varepsilon)) \le \exp(-c\varepsilon^2 N\delta).$$
 (32)

On $\operatorname{Bad}_k(\varepsilon)^c$ we have $\underline{m}_k \geq T(1-\varepsilon)N\delta$, hence

$$\frac{1}{\underline{m}_k} \ = \ \frac{1}{\underline{m}_k} \, \mathbf{1}_{\mathrm{Bad}_k(\varepsilon)^c} \ + \ \frac{1}{\underline{m}_k} \, \mathbf{1}_{\mathrm{Bad}_k(\varepsilon)} \ \le \ \frac{1}{T(1-\varepsilon)N\delta} \, \mathbf{1}_{\mathrm{Bad}_k(\varepsilon)^c} \ + \ \frac{1}{T} \, \mathbf{1}_{\mathrm{Bad}_k(\varepsilon)}.$$

Taking $\mathbb{E}_{A,L}$ and using (32),

$$\mathbb{E}_{\mathsf{A},\mathsf{L}}\left[\frac{1}{m_k}\right] \leq \frac{1}{T(1-\varepsilon)N\delta} + \frac{1}{T}e^{-c\varepsilon^2N\delta}. \tag{33}$$

Averaging (33) over k and using linearity,

$$\mathbb{E}_{\mathsf{A},\mathsf{L}}\left[\frac{1}{K}\sum_{k=1}^{K}\frac{1}{\underline{m}_{k}}\right] \leq \frac{1}{T(1-\varepsilon)N\delta} + \frac{1}{T}e^{-c\varepsilon^{2}N\delta}.$$
(34)

Taking $\mathbb{E}_{A,L}$ on both sides of (31) and using (34) (and absorbing the fixed $\log(2/\delta_0)$ into constants) gives

$$\mathbb{E}_{\mathsf{A},\mathsf{L}}\big[\mathcal{R}\big(\mathcal{D}\mid\mathsf{A},\mathsf{L}\big)\big] \leq \left(\frac{2}{\gamma}+C_1\right)\frac{B^2}{\gamma\,T(1-\varepsilon)N\delta} + C_2\,\frac{\sigma^2\,d_\lambda}{M} + C_3\,B^2\,\lambda + \left(\frac{2}{\gamma}+C_1\right)\frac{B^2}{\gamma\,T}\,e^{-c\,\varepsilon^2N\delta}. \tag{35}$$

For user k, if \mathcal{S}_k^{\star} is an essential set of size r_k , then the probability that a fixed coordinate in \mathcal{S}_k^{\star} is never both computed and linked across the N servers is at most $(1 - \gamma \delta)^N \leq e^{-\gamma N \delta}$. A union bound over \mathcal{S}_k^{\star} yields

Pr (coverage miss for user
$$k$$
) $\leq r_k e^{-\gamma N\delta}$.

Averaging over users,

$$\frac{1}{K} \sum_{k=1}^{K} \Pr\left(\text{coverage miss for user } k\right) \leq r_{\text{avg}} e^{-\gamma N \delta}.$$

By Lemma 5, the contribution of these miss events to the annealed risk is bounded (up to absolute constants) by $r_{\text{avg}}e^{-\gamma N\delta}$. Adding this term to (35) and absorbing the exponentially small $\frac{B^2}{\gamma T}e^{-c\varepsilon^2N\delta}$ term into $C_{\star}e^{-c\varepsilon^2N\delta}$ yields the annealed upper bound (16).

b) Part II (Converse): Conditionally on (A, L), Lemma 4 (per-user spectral tail) gives

$$\inf_{\text{schemes with } \leq m_k \text{ scalars}} \mathbb{E}_x[\|\widehat{F}_k(x) - F_k(x)\|_2^2] \geq B^2 \sum_{j>m_k} \lambda_j.$$

Taking $\mathbb{E}_{\mathsf{A},\mathsf{L}}$ and applying Jensen to $f(m) \triangleq \sum_{j>m} \lambda_j$ (convex on \mathbb{N}) yields

$$\inf_{\mathcal{D}} \mathbb{E}_{\mathsf{A},\mathsf{L}} \mathbb{E}_x \big[\| \widehat{F}_k(x) - F_k(x) \|_2^2 \big] \ \geq \ B^2 \sum_{j > m_k^{\mathrm{avg}}} \lambda_j, \qquad m_k^{\mathrm{avg}} = T N \delta.$$

For coverage, if $\gamma N\delta \lesssim \log(r_{\rm avg})$, the average miss probability is bounded away from zero, and Lemma 5 implies a constant floor c'>0 in the annealed risk, producing the indicator term in the theorem statement. Combining the spectral tail with the coverage threshold proves the annealed lower bound. This completes the proof.

V. Comparison

To evaluate our novel achievable scheme, we will compare our results with Theorem 2 of [8], under the same asymptotic conditions on the desired target functions. In particular, to embody the same conditions as Theorem 2 of [8], we assume that the output subfunctions are linear and isotropic, and then apply the achievable scheme of Theorem 1 using the general RKHS framework developed earlier, together with Lemma 2 (kernel approximation error) and Lemma 3 (ridge risk decomposition). This specialization allows us to clearly isolate the spectral mechanism that governs the error and to compare our scheme with the benchmark Marchenko–Pastur (MP) law, highlighting how the proposed achievable scheme performs asymptotically better than that of tessellated distributed computing. Throughout this comparison, we adopt the same limit order as in Theorem 2 of [8]:

¹This uses per-server masks/links fixed across the T shots. If masks are independently redrawn each shot, the miss probability becomes $(1 - \gamma \delta)^{NT} \leq e^{-\gamma N \delta T}$, further strengthening the bound.

- The input features are isotropic: $w(X) \in \mathbb{R}^L$ with $\mathbb{E}[w(X)] = 0$ and $\mathbb{E}[w(X)w(X)^\top] = I_L$.
- The ridge estimator is trained in the noiseless, infinite-sample limit: training sample size $M \to \infty$ and ridge parameter $\lambda \downarrow 0$.
- The system dimensions (K, N, L) grow large with fixed ratios

$$\gamma = \Gamma/L, \qquad \delta = \Delta/K, \qquad R = K/N.$$

Now consider linearly separable targets for K users

$$F(x) = \mathbf{F} \mathbf{w}(x) \in \mathbb{R}^K, \quad \mathbf{F} \in \mathbb{R}^{K \times L},$$

under the isotropic model described above. A linear scheme with computation/communication matrices $\mathbf{E} \in \mathbb{R}^{NT \times L}$ and $\mathbf{D} \in \mathbb{R}^{K \times NT}$ (supported by the bi-adjacency matrices of (A, L)) reconstructs $\widehat{F}(x) = \mathbf{DEw}(x)$. Recall the quenched population risk for a fixed topology (A, L) (Def. (7)):

$$\mathcal{R}(\mathcal{D} \mid \mathsf{A}, \mathsf{L}) = \mathbb{E}_x \left[\frac{1}{K} \sum_{k=1}^K \|\widehat{F}_k(x) - F_k(x)\|_2^2 \right].$$

In the same linear setting, TDC's normalized distortion (cf. [8]) is

$$D_{\text{TDC}} = \frac{1}{KL} \mathbb{E}_{\mathbf{F}, \mathbf{w}} \left[\min_{\mathbf{D}, \mathbf{E}} \| \mathbf{D} \mathbf{E} - \mathbf{F} \|_F^2 \right]. \tag{36}$$

When both sides are restricted to the same class of linear designs supported by (A, L), a direct comparison gives

$$D_{\text{TDC}} = \frac{1}{L} \mathcal{R}(\mathcal{D} \mid \mathsf{A}, \mathsf{L}). \tag{37}$$

We will show that in this limit, Lemma 3 reduces the error to the spectral projection loss of the Gram operator $G_{A,L} = \mathbb{E}[\Phi(X)\Phi(X)^{\top}]$, while Lemma 2 ensures the Monte-Carlo kernel error vanishes. Thus the quenched distortion is determined entirely by the empirical spectrum of $G_{A,L}$.

To be more precise, fix a user k. The (Γ, Δ) -regular topology $(A, L)^1$ determines (i) the *computation* supports of size Γ per encoded row and (ii) the *communication* pattern that routes T encoded shots per server to user k with per-shot indegree Δ on average. Stack the m_k scalars received by user k (over all servers and shots) into the feature map

$$\Phi_k(x) \in \mathbb{R}^{m_k}, \qquad \Phi_k(x) = E_k w(x),$$

where $E_k \in \mathbb{R}^{m_k \times L}$ is supported by the bi-adjacency matrices of (A, L) (rows have support size Γ). Note that, in this linear and isotropic specialization, the general Random Fourier Feature (RFF) construction used in the RKHS framework admits a simple linear limit. Recall that for a shift-invariant

¹A pair (A, L) is said to be (Γ, Δ) -regular if every server $n \in [N]$ satisfies $|S_n| = \Gamma$ and $|T_n| = \Delta$.

kernel K(x, x') = k(x - x'), Bochner's theorem ensures the existence of a nonnegative spectral density $p(\omega)$ such that

$$K(x, x') = \int_{\mathbb{R}^d} e^{j \,\omega^\top (x - x')} \, p(\omega) \, d\omega = \mathbb{E}_{\omega \sim p(\omega)} [\cos(\omega^\top (x - x'))].$$

Sampling frequencies $\omega_i \sim p(\omega)$ and random phases $b_i \sim \text{Unif}[0, 2\pi]$ yields the RFF embedding

$$\Phi(x) = \frac{1}{\sqrt{m}} \begin{bmatrix} \sqrt{2}\cos(\omega_1^\top x + b_1) \\ \vdots \\ \sqrt{2}\cos(\omega_m^\top x + b_m) \end{bmatrix}, \qquad K(x, x') \approx \Phi(x)^\top \Phi(x').$$

When the kernel bandwidth becomes large (for instance in the Gaussian kernel $K(x, x') = \exp(-\|x - x'\|^2/2\sigma^2)$ as $\sigma \to \infty$), the spectral measure $p(\omega)$ concentrates around $\omega = 0$, and we may linearize $\cos(\omega_i^{\mathsf{T}} x + b_i)$ around the origin:

$$\cos(\omega_i^{\top} x + b_i) = \cos(b_i) - \sin(b_i) \omega_i^{\top} x + O(\|\omega_i^{\top} x\|^2).$$

After rescaling, the random feature vector becomes approximately linear in x, with covariance $\mathbb{E}[\Phi(x)\Phi(x')^{\top}] \approx x^{\top}x'I_m/m$. Formally, taking the linear kernel limit $K(x,x') = x^{\top}x'$ corresponds to the degenerate spectral measure $p(\omega) = \sum_{\ell=1}^{d} \delta(\omega - e_{\ell})$, so that the RFF map reduces exactly to the identity:

$$\Phi(x) = [x_1, x_2, \dots, x_d]^{\top} = x.$$

In this limit, we model the random feature vector as an isotropic embedding $w(x) \sim \mathcal{N}(0, I_L)$ satisfying $\mathbb{E}[w(x)w(x')^{\top}] = K(x, x') = x^{\top}x'$. Hence, the relation $\Phi_k(x) = E_k w(x)$ simply expresses that user k has access to an encoded subset of the global RFF coordinates, with the support pattern of E_k determined by the computation and link topology (A, L); each nonzero entry of E_k indicates a subfunction index that is both computed and communicated to user k. Even when the underlying kernel reduces to the linear case $K(x, x') = x^{\top}x'$ so that the associated feature map becomes the identity and the random feature vector satisfies $w(x) \sim \mathcal{N}(0, I_L)$, the encoding matrices $\{E_k\}$ remain nontrivial. Indeed, E_k does not arise from the kernel itself but from the distributed system topology and resource constraints: it specifies which subset or linear combination of the L orthogonal subfunction outputs is both computed and communicated to user k. Formally,

$$E_k(\ell,j) \neq 0 \iff \exists n \in [N] \text{ s.t. } j \in \mathcal{A}_n, \ k \in \mathcal{T}_n,$$

where \mathcal{A}_n and \mathcal{T}_n denote, respectively, the computation and link supports of server n. Hence, even though the global covariance $\mathbb{E}[w(x)w(x')^{\top}] = K(x,x') = x^{\top}x'$ is identity, each user observes only the projected feature vector $\Phi_k(x) = E_k w(x)$ whose covariance $G_k = E_k E_k^{\top}$ has rank limited by the

normalized computation and communication budgets. Only in the fully centralized regime ($\gamma = \delta = 1$), where every server computes and transmits all subfunctions to all users, does $E_k = I_L$ and the distortion vanish. Under isotropy, $\mathbb{E}[w] = 0$ and $\mathbb{E}[ww^{\top}] = I_L$, the population Gram operator seen by the user is

$$G_k \triangleq \mathbb{E}[\Phi_k(X)\Phi_k(X)^{\top}] = E_k E_k^{\top} \succeq 0. \tag{38}$$

Let $\{\xi_{k,(i)}\}_{i=1}^{m_k}$ be the eigenvalues of G_k in nonincreasing order, and let $\mu_k \triangleq \frac{1}{m_k} \sum_{i=1}^{m_k} \delta_{\xi_{k,(i)}}$ be its empirical spectral distribution (ESD). For the linear/isotropic comparison below, we may drop the subscript k when no confusion arises. The above is summarized in the following proposition:

Proposition 1. Work under the setup and assumptions used in Theorem 1: (i) fixed (A, L) (quenched); (ii) linear/isotropic inputs $w(X) \in \mathbb{R}^L$ with $\mathbb{E}[w] = 0$ and $\mathbb{E}[ww^\top] = I_L$; (iii) feature map for user k given by $\Phi_k(x) = E_k w(x) \in \mathbb{R}^{m_k}$ with E_k supported by (A, L). Consider the ridge predictor trained with M i.i.d. samples and penalty $\lambda > 0$:

$$\widehat{\beta}_{M,\lambda} \in \arg\min_{\beta \in \mathbb{R}^{m_k}} \frac{1}{M} \sum_{i=1}^{M} \left(\beta^\top \Phi_k(x_i) - F_k(x_i) \right)^2 + \lambda \|\beta\|_2^2, \quad \widehat{F}_{M,\lambda}(x) = \widehat{\beta}_{M,\lambda}^\top \Phi_k(x).$$

In the noiseless, infinite-sample limit $(M \to \infty \text{ and } \lambda \downarrow 0)$, the trained decoder converges in $L_2(\mathbb{P}_X)$ to the orthogonal projector P onto $\operatorname{span}\{\Phi_k(x): x \in \mathcal{X}\} \subset L_2(\mathbb{P}_X)$:

$$\widehat{F}_{M,\lambda} \xrightarrow{L_2(\mathbb{P}_X)} PF_k, \qquad P: L_2(\mathbb{P}_X) \to \overline{\operatorname{span}\{\Phi_k(\cdot)\}}.$$

Consequently, letting $G_k = \mathbb{E}[\Phi_k(X)\Phi_k(X)^{\top}] \succeq 0$ with ordered eigenvalues $\xi_{(1)} \geq \cdots \geq \xi_{(m_k)} \geq 0$ and empirical spectral law $\mu = \frac{1}{m_k} \sum_{i=1}^{m_k} \delta_{\xi_{(i)}}$, the 1/(KL)-normalized quenched distortion of our linear scheme equals the energy discarded by truncation at mass $\kappa = 1 - m_{\text{eff}}$:

$$D_{\text{MUDC}}^{\mathbf{q}}(\mathsf{A},\mathsf{L}) = \frac{1}{L} \sum_{i=m_k - \lceil \kappa m_k \rceil + 1}^{m_k} \xi_{(i)} = \int_0^{\kappa} Q_{\mu}^{\downarrow}(u) \, du, \tag{39}$$

where Q_{μ}^{\downarrow} is the lower-tail quantile of μ and $m_{\mathrm{eff}} = \frac{T\gamma N}{K}$.

Proof of Proposition 1 is provided in Appendix F. In what follows, we argue that under disjoint and balanced supports (the structural assumption of TDC), the Gram spectrum converges to the Marchenko–Pastur law $MP_{\lambda'}$ with aspect ratio $\lambda' = \delta K/(\gamma L) = \Delta/\Gamma$. The corresponding truncated first moment $\Phi_{MP,\lambda'}$ was shown in [8] to serve as both an achievability result (for TDC) and a converse within that class. We then examine how deviations from the disjoint-support assumption—through overlapping subfunction assignments or nonuniform link topologies—affect performance, and to what extent such structures can yield gains or losses in terms of the normalized error.

In particular, we compare $D_{\mathrm{MUDC}}^{\mathrm{q}}$ to the Marchenko–Pastur (MP) envelope at the same budgets 1 .

$$\lambda' \triangleq \frac{\delta K}{\gamma L} = \frac{\Delta}{\Gamma}, \qquad r = (1 - \sqrt{\lambda'})^2, \quad b = (1 + \sqrt{\lambda'})^2.$$
 (40)

Let $f_{\text{MP},\lambda'}$ and $F_{\text{MP},\lambda'}$ be the MP density and CDF on [r,b]. The MP truncation threshold t is defined implicitly by

$$F_{\text{MP},\lambda'}(t) = \kappa = 1 - \frac{T\gamma N}{K}. \tag{41}$$

The corresponding truncated first moment (the MP benchmark) is

$$\Phi_{\mathrm{MP},\lambda'}(t,r) \triangleq \int_{r}^{t} x \, f_{\mathrm{MP},\lambda'}(x) \, dx = \int_{0}^{\kappa} Q_{\mathrm{MP},\lambda'}^{\downarrow}(u) \, du. \tag{42}$$

Given a fixed (Γ, Δ) -regular topology (A, L), we ask: how close is the quenched distortion $D^q_{\text{MUDC}}(A, L)$, employing the achievable approach of this paper, to the MP envelope $\Phi_{\text{MP},\lambda'}$? The difference

$$G^{q}(A, L) = \Phi_{MP, \lambda'} - D_{MUDC}^{q}(A, L)$$

is what we call the quenched MP–gap. It measures the extent to which a given assignment/link structure "wastes" spectral mass compared to the MP benchmark. In what follows, we see that this gap is always nonnegative and vanishes for disjoint-and-balanced tessellations, while overlap or aliasing can increase it strictly. With this in place, we proceed to the formal statement giving the exact gap representation and tight bounds.

Theorem 3. Work in the linear/isotropic setting and fix a (Γ, Δ) -regular topology (A, L). Let L be the ambient dimension for the user, and set

$$m_{\text{eff}} \triangleq \min \left\{ 1, \frac{T\gamma N}{K} \right\}, \qquad \kappa \triangleq 1 - m_{\text{eff}}.$$

Let $G_{\mathsf{A},\mathsf{L}} = \mathbb{E}[\Phi(X)\Phi(X)^{\top}] \in \mathbb{R}^{L \times L}$ be the user Gram operator and $\mu_{\mathsf{A},\mathsf{L}} \equiv \frac{1}{L} \sum_{i=1}^{L} \delta_{\xi_{(i)}}$ its empirical spectral law with eigenvalues $\xi_{(1)} \geq \cdots \geq \xi_{(L)} \geq 0$. Throughout, the eigenvalues are ordered in descending order, and the quantile function Q^{\downarrow}_{μ} is defined accordingly as the nonincreasing (right-continuous) inverse of the CDF F_{μ} , i.e., $Q^{\downarrow}_{\mu}(u) = \inf\{x : F_{\mu}(x) \geq u\}$. Define the lower-tail quantile $Q^{\downarrow}_{\mu}(u) \triangleq \inf\{x : F_{\mu}(x) \geq u\}$ for $u \in [0, 1]$. The 1/(KL)-normalized quenched distortion of our linear scheme is

$$D_{\mathrm{MUDC}}^{\mathrm{q}}(\mathsf{A},\mathsf{L}) \ = \ \frac{1}{L} \sum_{i=L-\lceil \kappa L \rceil+1}^{L} \xi_{(i)} \ = \ \int_{0}^{\kappa} Q_{\mu_{\mathsf{A},\mathsf{L}}}^{\downarrow}(u) \, du.$$

¹Notation: we reserve λ for ridge; we write λ' for the MP aspect ratio.

Let $\lambda' = \delta K/(\gamma L) = \Delta/\Gamma$, let $MP_{\lambda'}$ be the Marchenko-Pastur law with that aspect ratio, and define its lower-tail quantile $Q_{MP,\lambda'}^{\downarrow}$ and $CDF\ F_{MP,\lambda'}$. Let $t\ solve\ F_{MP,\lambda'}(t) = \kappa$ and define the MP benchmark

$$\Phi_{\mathrm{MP},\lambda'}(\kappa) \triangleq \int_0^{\kappa} Q_{\mathrm{MP},\lambda'}^{\downarrow}(u) \, du = \int x \, \mathbf{1}_{\{x \leq t\}} \, d\mathrm{MP}_{\lambda'}(x).$$

Define the quenched MP-gap

$$G^{q}(A, L) \triangleq \Phi_{MP, \lambda'}(\kappa) - D_{MUDC}^{q}(A, L).$$

Then:

(a) Exact gap representation.

$$G^{\mathbf{q}}(\mathsf{A},\mathsf{L}) = \int_{0}^{\kappa} \left(Q_{\mathsf{MP},\lambda'}^{\downarrow}(u) - Q_{\mu_{\mathsf{A},\mathsf{L}}}^{\downarrow}(u) \right) du. \tag{43}$$

(b) Nonnegativity and a robust lower bound. Assume the coverage and eigen-tail constraints of Lemmas 4–5 (Section IV) hold, which imply the MP upper envelope on truncated first moments:

$$\int_0^{\kappa} Q_{\mu_{\mathsf{A},\mathsf{L}}}^{\downarrow}(u) \, du \, \leq \, \int_0^{\kappa} Q_{\mathrm{MP},\lambda'}^{\downarrow}(u) \, du.$$

Then $G^{q}(\mathsf{A},\mathsf{L}) \geq 0$, with equality iff $Q_{\mu_{\mathsf{A},\mathsf{L}}}^{\downarrow} = Q_{\mathrm{MP},\lambda'}^{\downarrow}$ a.e. on $[0,\kappa]$. Moreover, if for some measurable $U \subset [0,\kappa]$ with $|U| = \eta > 0$ and some $\alpha > 0$ one has $Q_{\mu_{\mathsf{A},\mathsf{L}}}^{\downarrow}(u) \leq Q_{\mathrm{MP},\lambda'}^{\downarrow}(u) - \alpha$ for all $u \in U$, then

$$G^{q}(A, L) \geq \alpha \eta.$$
 (44)

(c) Simple upper bound. If the supports of both spectra lie in [0,b] for some $b < \infty$ (e.g. $b = (1+\sqrt{\lambda'})^2$ in the classical MP setting), then

$$0 \le G^{\mathbf{q}}(\mathsf{A},\mathsf{L}) \le \Phi_{\mathrm{MP},\lambda'}(\kappa) \le b \kappa = b \Big(1 - \frac{T\gamma N}{K} \Big). \tag{45}$$

Remark 3. The nonnegativity of the MP-gap $G^{\mathbf{q}} \geq 0$ relies on the standard spectral dominance assumption: under disjoint and balanced supports (the TDC regime), the empirical spectrum of $E_k E_k^{\mathsf{T}}$ converges to the Marchenko-Pastur law, which upper-bounds the truncated first moment among all (Γ, Δ) -regular topologies. Hence, $G^{\mathbf{q}} > 0$ indicates that the proposed masked-RFF-based design achieves strictly higher spectral energy retention than the TDC baseline when the topology departs from perfect tessellation.

Proof of Theorem 3 is provided in Appendix G. The quenched MP-gap G^q quantifies how much the empirical lower spectral tail of the user Gram matrix *improves upon* the Marchenko-Pastur (MP) benchmark under the same budgets (γ, δ, T) . It represents the *area* between the MP and empirical lower-tail quantiles over the discarded spectral mass $\kappa = 1 - T\gamma N/K$, thereby measuring the additional spectral energy preserved by our scheme beyond the MP prediction. Under disjoint and balanced tessellations (the TDC structural condition), the empirical spectral law converges to $MP_{\lambda'}$, so the truncated first moment (42) equals the empirical lower-tail mean and $G^q = 0$. In this regime, our achievable scheme *matches* the optimal performance of TDC, confirming its consistency with the best-known spectral benchmark.

More importantly, when the system departs from strict disjointness—through partially overlapping computation supports or nonuniform link patterns—our proposed achievable scheme remains valid and continues to yield explicit performance guarantees. Unlike the TDC design, which fundamentally requires disjoint and balanced partitions, the present scheme naturally extends to arbitrary (Γ, Δ) -regular topologies and captures the additional gain through the MP-gap characterization. This reveals that, even for linearly separable and isotropic targets, the proposed framework can outperform tessellated distributed computing whenever the system structure deviates from perfect tessellation, by exploiting partial overlaps more efficiently and preserving a larger fraction of spectral energy. Any overlap or aliasing in computation masks or link patterns (for example, repeated subfunction supports across servers or hub-like links) tends to depress the empirical lower-tail quantile $Q_{\text{MP},\lambda'}^{\downarrow}$ below its MP counterpart $Q_{\text{MP},\lambda'}^{\downarrow}$ on a set of nonzero measure, thus reducing the discarded spectral mass and yielding a strictly positive gap $G^{\text{q}} > 0$ as given by (44). Hence, the proposed scheme not only explains but also quantifies this improvement through the analytical MP-gap measure, enabling a systematic spectral comparison across arbitrary network structures—something that was not possible in the purely tessellated model.

The envelope bound (45) further shows that increasing T, γ , or N reduces κ and thereby pushes the effective spectrum closer to full coverage, while increasing δ (for fixed γ, L, K) decreases λ' and tightens the MP bulk, enhancing spectral efficiency. In summary, disjoint-and-balanced topologies reproduce the MP benchmark (yielding $G^{q} = 0$), whereas overlapping or imbalanced designs can achieve strictly positive MP–gaps that reveal super-MP performance. The proposed achievable scheme remains applicable and provably near-optimal in all such cases, offering a unified spectral characterization that not only generalizes but also extends the tessellated distributed computing framework.

VI. CONCLUSION

This work introduces the *General Multi-User Distributed Computing (GMUDC)* framework, a unified learning-theoretic formulation that characterizes the joint trade-off between computation, communication, and accuracy across heterogeneous multi-user, multi-server systems. Unlike existing distributed-computation models [8], [30], GMUDC requires no separability assumption on users,

subfunctions, or data partitions: the only structural assumption is that each target function belongs to a bounded Reproducing-Kernel Hilbert Space (RKHS) associated with a shift-invariant kernel, encompassing both linear and smooth nonlinear mappings such as Gaussian, Laplacian, and polynomial kernels. This general formulation remains valid for arbitrary server—user assignment topologies, thereby unifying structured and unstructured distributed systems within a single analytical model. By interpreting encoding and decoding as functional regression operators in the RKHS, GMUDC bridges classical algebraic computing architectures and modern distributed-learning formulations through a common kernel-ridge inference law. An achievable design based on masked Random Fourier Features (RFFs) satisfies both computation and communication budgets, yielding explicit quenched and annealed risk bounds that expose a sharp computation—communication—accuracy trade-off and an exponential coverage phase transition. The framework establishes a spectral—coverage duality and a Marchenko—Pastur (MP) gap law, revealing how network topology and link reuse govern spectral efficiency. These principles provide theoretical guidance for distributed and federated learning under resource constraints, with direct applications to aeronautical and aerospace networks such as distributed Kalman filtering, consensus estimation, and cooperative trajectory optimization.

Future Research Directions

- Adaptive and Hierarchical GMUDC. Extend the current single-layer model to hierarchical
 or time-varying topologies, allowing adaptive reallocation of computation and communication
 budgets in response to network dynamics.
- Learning-Integrated Distributed Optimization. Couple GMUDC with gradient-coded and federated optimization algorithms to analyze convergence—risk trade-offs jointly with communication cost, moving toward a unified "coded-learning" theory.
- Spectral Topology Design. Use the MP-gap characterization to construct topology-aware allocation schemes that minimize spectral loss for given (Γ, Δ, T) , yielding provably optimal connectivity graphs.
- Noisy and Adversarial Regimes. Generalize the current noiseless setup to stochastic or adversarial servers, extending the spectral-coverage converse to uncertainty-aware distributed computing.

References

[1] J. Verbraeken, M. Wolting, J. Katzy, J. Kloppenburg, T. Verbelen, and J. S. Rellermeyer, "A survey on distributed machine learning," *ACM Computing Surveys (CSUR)*, vol. 53, no. 2, pp. 1–33, 2020.

- [2] S. Ulukus, S. Avestimehr, M. Gastpar, S. Jafar, R. Tandon, and C. Tian, "Private retrieval, computing and learning: Recent progress and future challenges," *IEEE Journal on Selected Areas in Communications*, 2022.
- [3] S. Wang, J. Liu, N. Shroff, and P. Yang, "Fundamental limits of coded linear transform," in Proceedings of the Twenty-Second International Conference on Artificial Intelligence and Statistics, ser. Proceedings of Machine Learning Research, K. Chaudhuri and M. Sugiyama, Eds., vol. 89. PMLR, 16–18 Apr 2018, pp. 577–585. [Online]. Available: https://proceedings.mlr.press/v89/wang19a.html
- [4] S. Li, M. A. Maddah-Ali, Q. Yu, and A. S. Avestimehr, "A fundamental tradeoff between computation and communication in distributed computing," *IEEE Transactions on Information Theory*, vol. 64, no. 1, pp. 109–128, 2017.
- [5] Q. Yu, M. Maddah-Ali, and S. Avestimehr, "Polynomial codes: an optimal design for high-dimensional coded matrix multiplication," *Advances in Neural Information Processing Systems*, vol. 30, 2017.
- [6] A. Reisizadeh, S. Prakash, R. Pedarsani, and A. S. Avestimehr, "Codedreduce: A fast and robust framework for gradient aggregation in distributed learning," *IEEE/ACM Transactions on Networking*, 2021.
- [7] M. Chen, D. Gündüz, K. Huang, W. Saad, M. Bennis, A. V. Feljan, and H. V. Poor, "Distributed learning in wireless networks: Recent progress and future challenges," *IEEE Journal on Selected Areas in Communications*, vol. 39, no. 12, pp. 3579–3605, 2021.
- [8] A. Khalesi and P. Elia, "Tessellated distributed computing," *IEEE Transactions on Information Theory*, vol. 71, no. 6, pp. 4754–4784, 2025.
- [9] D. Malak and M. Médard, "A distributed computationally aware quantizer design via hyper binning," *IEEE Transactions on Signal Processing*, vol. 71, pp. 76–91, 2023.
- [10] D. P. Woodruff *et al.*, "Sketching as a tool for numerical linear algebra," Foundations and Trends® in Theoretical Computer Science, vol. 10, no. 1–2, pp. 1–157, 2014.
- [11] T. Jahani-Nezhad and M. A. Maddah-Ali, "Codedsketch: A coding scheme for distributed computation of approximated matrix multiplication," *IEEE Transactions on Information Theory*, vol. 67, no. 6, pp. 4185–4196, 2021.
- [12] W.-T. Chang and R. Tandon, "Random sampling for distributed coded matrix multiplication," in ICASSP 2019 -2019 IEEE International Conference on Acoustics, Speech and Signal Processing (ICASSP), 2019, pp. 8187–8191.
- [13] N. Charalambides, M. Pilanci, and A. O. Hero, "Approximate weighted CR coded matrix multiplication," in ICASSP 2021 - 2021 IEEE International Conference on Acoustics, Speech and Signal Processing (ICASSP), 2021, pp. 5095–5099.
- [14] V. Gupta, S. Wang, T. Courtade, and K. Ramchandran, "Oversketch: Approximate matrix multiplication for the cloud," in 2018 IEEE International Conference on Big Data (Big Data), 2018, pp. 298–304.
- [15] N. S. Ferdinand and S. C. Draper, "Anytime coding for distributed computation," in 2016 54th Annual Allerton Conference on Communication, Control, and Computing (Allerton), 2016, pp. 954–960.
- [16] J. Zhu, Y. Pu, V. Gupta, C. Tomlin, and K. Ramchandran, "A sequential approximation framework for coded distributed optimization," in 2017 55th Annual Allerton Conference on Communication, Control, and Computing (Allerton), 2017, pp. 1240–1247.
- [17] T. Jahani-Nezhad and M. A. Maddah-Ali, "Berrut approximated coded computing: Straggler resistance beyond polynomial computing," *IEEE Transactions on Pattern Analysis and Machine Intelligence*, vol. 45, no. 1, pp. 111–122, 2023.
- [18] H. Jeong, A. Devulapalli, V. R. Cadambe, and F. P. Calmon, " ϵ -approximate coded matrix multiplication is

- nearly twice as efficient as exact multiplication," *IEEE Journal on Selected Areas in Information Theory*, vol. 2, no. 3, pp. 845–854, 2021.
- [19] R. Ji, A. Heidarzadeh, and K. R. Narayanan, "Sparse random Khatri-Rao product codes for distributed matrix multiplication," in 2022 IEEE Information Theory Workshop (ITW), 2022, pp. 416–421.
- [20] M. Rudow, N. Charalambides, A. O. Hero, and K. Rashmi, "Compression-informed coded computing," in 2023 IEEE International Symposium on Information Theory (ISIT), 2023, pp. 2177–2182.
- [21] N. Agrawal, Y. Qiu, M. Frey, I. Bjelakovic, S. Maghsudi, S. Stanczak, and J. Zhu, "A learning-based approach to approximate coded computation," in 2022 IEEE Information Theory Workshop (ITW), 2022, pp. 600–605.
- [22] T. Jahani-Nezhad and M. A. Maddah-Ali, "Optimal communication-computation trade-off in heterogeneous gradient coding," *IEEE Journal on Selected Areas in Information Theory*, vol. 2, no. 3, pp. 1002–1011, 2021.
- [23] —, "Codedsketch: Coded distributed computation of approximated matrix multiplication," in 2019 IEEE International Symposium on Information Theory (ISIT), 2019, pp. 2489–2493.
- [24] N. Omidvar, S. M. Hosseini, and M. A. Maddah-Ali, "Hybrid-order distributed sgd: Balancing communication overhead, computational complexity, and convergence rate for distributed learning," *Neurocomputing*, vol. 599, p. 128020, 2024.
- [25] P. Moradi, B. Tahmasebi, and M. Maddah-Ali, "Coded computing for resilient distributed computing: A learning-theoretic framework," in Advances in Neural Information Processing Systems (NeurIPS), 2024.
- [26] P. Moradi and M. Maddah-Ali, "General coded computing in a probabilistic straggler regime," arXiv preprint arXiv:2502.00645, 2025.
- [27] P. Moradi, H. Akbarinodehi, and M. Maddah-Ali, "General coded computing: Adversarial settings," arXiv preprint arXiv:2502.08058, 2025.
- [28] K. Wan, H. Sun, M. Ji, and G. Caire, "Distributed linearly separable computation," *IEEE Transactions on Information Theory*, 2021.
- [29] A. Khalesi and P. Elia, "Perfect multi-user distributed computing," in *IEEE International Symposium on Information Theory (ISIT)*, Athens, Greece, 2024, pp. 1349–1354.
- [30] —, "Multi-user linearly-separable distributed computing," 2022. [Online]. Available: https://arxiv.org/abs/2206.11119
- [31] A. Ramamoorthy, L. Tang, and P. O. Vontobel, "Universally decodable matrices for distributed matrix-vector multiplication," in 2019 IEEE International Symposium on Information Theory (ISIT), 2019, pp. 1777–1781.
- [32] M. Ye and E. Abbe, "Communication-computation efficient gradient coding," in *International Conference on Machine Learning*. PMLR, 2018, pp. 5610–5619.
- [33] N. Raviv, I. Tamo, R. Tandon, and A. G. Dimakis, "Gradient coding from cyclic MDS codes and expander graphs," *IEEE Transactions on Information Theory*, vol. 66, no. 12, pp. 7475–7489, 2020.
- [34] Q. Yu, M. A. Maddah-Ali, and A. S. Avestimehr, "Straggler mitigation in distributed matrix multiplication: Fundamental limits and optimal coding," *IEEE Transactions on Information Theory*, vol. 66, no. 3, pp. 1920–1933, 2020.
- [35] P. Kairouz, H. B. McMahan, B. Avent *et al.*, "Advances and open problems in federated learning," *Foundations and Trends in Machine Learning*, vol. 14, no. 1–2, pp. 1–210, 2021.
- [36] J. Park, Y. Y. Kim, T. Kim, and S.-H. Choi, "Communication-efficient distributed kernel regression with adaptive compression," *IEEE Transactions on Neural Networks and Learning Systems*, vol. 32, no. 11, pp. 4751–4763, 2021.

- [37] J. D. Lee, Q. Liu, and Y. Sun, "Distributed ridge regression: optimal rates and communication trade-offs," *Annals of Statistics*, vol. 49, no. 1, pp. 77–102, 2021.
- [38] R. Olfati-Saber, J. A. Fax, and R. M. Murray, "Consensus and cooperation in networked multi-agent systems," *Proceedings of the IEEE*, vol. 95, no. 1, pp. 215–233, 2007.
- [39] F. S. Cattivelli and A. H. Sayed, "Diffusion strategies for distributed kalman filtering and smoothing," *IEEE Transactions on Automatic Control*, vol. 55, no. 9, pp. 2069–2084, 2010.
- [40] R. W. Beard, T. W. McLain, M. A. Goodrich, and E. P. Anderson, "Coordination of uavs via coupled dynamic models," Proceedings of the 2002 American Control Conference (ACC), pp. 2558–2563, 2002.
- [41] Q. Sun, Z. Lin, and H. Wang, "Distributed aerodynamic field estimation for multiple uavs using consensus-based filters," *Aerospace Science and Technology*, vol. 87, pp. 567–577, 2019.
- [42] Z. Li, Q. Sun, and Y. Zhang, "Decentralized cooperative estimation for spacecraft formation flying with communication delays," Acta Astronautica, vol. 175, pp. 220–232, 2020.
- [43] P. L. Bartlett and S. Mendelson, "Rademacher and gaussian complexities: Risk bounds and structural results," Journal of Machine Learning Research, vol. 3, pp. 463–482, 2002.
- [44] B. Schölkopf and A. J. Smola, Learning with Kernels: Support Vector Machines, Regularization, Optimization, and Beyond. Cambridge, MA: MIT Press, 2002, chapter 2, especially Sections 2.3–2.4 on RKHS and the reproducing property.
- [45] A. Berlinet and C. Thomas-Agnan, Reproducing Kernel Hilbert Spaces in Probability and Statistics. Springer, 2004, see Chapter 2 on Mercer kernels and integral operators.
- [46] A. Rudi and L. Rosasco, "Generalization properties of learning with random features," Advances in Neural Information Processing Systems, vol. 30, 2017. [Online]. Available: https://proceedings.neurips.cc/paper/2017/ hash/f7228da70fb28752fe384c1dd17c0c08-Abstract.html
- [47] H. Wendland, Scattered Data Approximation. Cambridge: Cambridge University Press, 2005, see chapter Positive definite and conditionally positive definite functions (Bochner & Schoenberg).
- [48] M. Mohri, A. Rostamizadeh, and A. Talwalkar, Foundations of Machine Learning, 2nd ed. Cambridge, MA: MIT Press, 2018, see chapter: Kernel Methods subsection on positive definite kernels and Gram matrices; explicitly notes Gram matrices are PSD, which applies to $G = \mathbb{E}[\Phi(X)\Phi(X)^{\top}]$.
- [49] T. Hastie, R. Tibshirani, and J. Friedman, The Elements of Statistical Learning: Data Mining, Inference, and Prediction, 2nd ed. New York: Springer, 2009, see chapters: Linear Methods for Regression (ridge; hat matrix) and Model Assessment and Selection (effective degrees of freedom $tr(S_{\lambda})$).
- [50] B. Schölkopf and A. J. Smola, Learning with Kernels: Support Vector Machines, Regularization, Optimization, and Beyond. Cambridge, MA: MIT Press, 2002.
- [51] A. Pinkus, *n-Widths in Approximation Theory*, ser. Ergebnisse der Mathematik und ihrer Grenzgebiete. Springer, 1985, vol. 93, see Chapter 1, especially sections 1.2–1.4 and Theorem 1.3.2.
- [52] B. Carl and I. Stephani, Entropy, Compactness and the Approximation of Operators, ser. Cambridge Tracts in Mathematics. Cambridge University Press, 1990, vol. 98, see Chapter 2, Sections 2.3, especially Corollary 2.3.2.
- [53] E. Novak and H. Woźniakowski, *Tractability of Multivariate Problems. Volume I: Linear Information*, ser. EMS Tracts in Mathematics. European Mathematical Society, 2008, vol. 6, see Chapter 4, Theorem 4.4.
- [54] R. Bhatia, Matrix Analysis, ser. Graduate Texts in Mathematics. New York: Springer, 1997, vol. 169.

Appendix A

Proof of Lemma 1

Proof. Let $u = \mathbf{w}(x)$ and $v = \mathbf{w}(x')$, and fix the mask $S \subseteq [L]$ with $|S| = \Gamma$ and $\gamma = \Gamma/L$. Write $\widetilde{\omega} = \omega \odot \mathbf{1}_S$ and

$$\phi_u \triangleq \phi(x; \omega, b, \mathcal{S}) = \sqrt{\frac{2}{\gamma}} \cos(\langle \widetilde{\omega}, u \rangle + b), \qquad \phi_v \triangleq \phi(x'; \omega, b, \mathcal{S}) = \sqrt{\frac{2}{\gamma}} \cos(\langle \widetilde{\omega}, v \rangle + b).$$

Set the single-atom kernel estimator $Z \triangleq \phi_u \phi_v$. We assume $|K| \leq 1$ and $\|\mathbf{w}(x)\|_2 \leq R$ a.s. Let $S \triangleq \langle \widetilde{\omega}, u - v \rangle$. Using the trigonometric identity $\cos(\alpha + b) \cos(\beta + b) = \frac{1}{2} \left[\cos(\alpha - \beta) + \cos(2b + \alpha + \beta) \right]$ and $\mathbb{E}_b[\cos(2b + \cdot)] = 0$, we get $\mathbb{E}_b[Z \mid \omega] = \frac{1}{\gamma} \cos S$. If $\widetilde{\omega}$ is sampled from the masked Bochner law, i.e., draw $\omega_S \sim \mu$ on \mathbb{R}^{Γ} and embed $(\omega_S, 0_{S^c})$, then Bochner's identity yields $\mathbb{E}_{\omega,b}[Z] = \frac{1}{\gamma} \mathbb{E}_{\widetilde{\omega}}[\cos S] = K(u, v)$. By the law of total variance, $\operatorname{Var}(Z) = \mathbb{E}[\operatorname{Var}_b(Z \mid \omega)] + \operatorname{Var}(\mathbb{E}_b[Z \mid \omega]) = \mathbb{E}[\operatorname{Var}_b(Z \mid \omega)] + \frac{1}{\gamma^2} \operatorname{Var}(\cos S)$. A direct computation shows $\mathbb{E}[\operatorname{Var}_b(Z \mid \omega)] \leq \frac{1}{2\gamma^2}$ (indeed $|\phi_u \phi_v| \leq 2/\gamma$ and the oscillatory term contributes at most $1/(2\gamma^2)$). Thus

$$Var(Z) \le \frac{1}{2\gamma^2} + \frac{1}{\gamma^2} Var(\cos S). \tag{46}$$

The cosine is 1-Lipschitz, hence for any random X, $Var(\cos X) \leq \mathbb{E}[(\cos X - \mathbb{E}\cos X)^2] \leq \mathbb{E}[(\cos X - \mathbb{E}\cos X)^2] \leq \mathbb{E}[X^2]$. Applying this with X = S,

$$\operatorname{Var}(\cos S) \leq \mathbb{E}[S^2] = (u-v)^{\top} \mathbb{E}[\widetilde{\omega}\widetilde{\omega}^{\top}] (u-v) = (u-v)^{\top} \Sigma_{\mathcal{S}}(u-v).$$

Let $\Sigma \triangleq \mathbb{E}[\omega\omega^{\top}]$ and note $\Sigma_{\mathcal{S}} \preceq \Sigma$ (PSD order). Because inputs live in the compact ball $\{u : ||u||_2 \leq R\}$, there exists a constant $C_{K,R} \in (0,\infty)$ such that, for all u,v,

$$(u-v)^{\top} \Sigma(u-v) \leq C_{K,R} \left(K(u,u) + K(v,v) - 2K(u,v) \right) = C_{K,R} V_K(u,v).^{1}$$
(47)

Therefore,

$$\mathbb{E}[S^2] = (u - v)^{\top} \Sigma_{\mathcal{S}}(u - v) \le (u - v)^{\top} \Sigma(u - v) \le C_{K,R} V_K(u, v).$$

Plug the bound on $Var(\cos S)$ into (46):

$$\operatorname{Var}(Z) \leq \frac{1}{2\gamma^2} + \frac{C_{K,R}}{\gamma^2} V_K(u,v). \tag{48}$$

¹Reason: write $\varphi(h) = \mathbb{E}[e^{i\langle\omega,h\rangle}]$ so that $K(u,v) = \varphi(u-v)$ with $\varphi(0) = 1$. Since $\int \|\omega\|_2^2 d\mu(\omega) < \infty$, φ is C^2 near 0 with $\nabla \varphi(0) = 0$ and $\nabla^2 \varphi(0) = -\Sigma$. Hence $1 - \varphi(h) = \frac{1}{2}h^{\top}\Sigma h + o(\|h\|^2)$ as $h \to 0$, which implies $\lim_{h\to 0} \frac{h^{\top}\Sigma h}{1-\varphi(h)} = 2$. On the compact set $\{h: \|h\| \le 2R\}$, the function $g(h) = \frac{h^{\top}\Sigma h}{1-\varphi(h)}$ is continuous and attains a finite maximum $C_{K,R}$. Substituting h = u - v gives (47).

Finally, the masked-feature normalization $\sqrt{2/\gamma}$ was chosen so that the single-atom variance inflates by a factor $1/\gamma$ relative to the unmasked atom (whose variance is $\lesssim V_K$). Grouping constants gives

$$Var(Z) \leq \frac{1}{2\gamma^2} + \frac{1}{\gamma} V_K(u, v),$$

i.e., (19) with $C_{\text{mask}} = 1$. If $\omega \sim \mu$ on \mathbb{R}^L and we truncate by $\widetilde{\omega} = \omega \odot \mathbf{1}_{\mathcal{S}}$, then second moments on \mathcal{S} match the masked-Bochner law:

$$\mathbb{E}[\widetilde{\omega}_i \widetilde{\omega}_j] = \begin{cases} \mathbb{E}[\omega_i \omega_j], & i, j \in \mathcal{S}, \\ 0, & \text{otherwise,} \end{cases}$$

so the bound in (48) persists with a possibly larger constant depending only on $\int \|\omega\|_2^2 d\mu(\omega)$ and R.¹ Thus there exists an absolute $C_{\text{mask}} \geq 1$ such that

$$\operatorname{Var}(Z) \leq \frac{1}{2\gamma^2} + \frac{C_{\text{mask}}}{\gamma} V_K(u, v).$$

Appendix B

Proof of Lemma 2

Proof. Fix a user k and a realization (A, L). For each received feature index $j \in [m_k]$ (corresponding to some (n, t) with $k \in \mathcal{T}_{n,t}$), define

$$\phi_j(x) \triangleq \sqrt{\frac{2}{\gamma}} \cos(\widetilde{\omega}_j^{\top} \mathbf{w}(x) + b_j), \qquad Z_j(x, x') \triangleq \phi_j(x) \phi_j(x'),$$

where $\widetilde{\omega}_j = \omega_j \odot \mathbf{1}_{\mathcal{S}_j}$ with $|\mathcal{S}_j| = \Gamma$, $\gamma = \Gamma/L$, and $b_j \sim \text{Unif}[0, 2\pi]$. The masked Monte Carlo (MC) kernel at user k is

$$\widetilde{K}_k(x, x') = \frac{1}{m_k} \sum_{j=1}^{m_k} Z_j(x, x').$$

¹The constant persists because the variance bound for $Z = \phi(x)\phi(x')$ is controlled (up to absolute factors) by the sub-Gaussian proxy of $S = \widetilde{\omega}^{\top}(u-v)$, which depends only on the covariance of $\widetilde{\omega}$ and on $||u-v||_2 \leq 2R$. When we truncate $\omega \sim \mu$ by $\widetilde{\omega} = \omega \odot \mathbf{1}_S$, the second moments on S are preserved, i.e., $\mathbb{E}[\widetilde{\omega}_i\widetilde{\omega}_j] = \mathbb{E}[\omega_i\omega_j]$ for $i,j \in S$ and 0 otherwise, so $\text{Var}(S) = (u-v)^{\top}\Sigma_S(u-v)$ with $\Sigma_S \preceq \Sigma = \mathbb{E}[\omega\omega^{\top}]$. By contraction/Lipschitz arguments for $\cos(\cdot)$, Var(Z) is bounded by a constant multiple of Var(S) (plus the bounded b-oscillation term), and hence by a constant multiple of $(u-v)^{\top}\Sigma_S(u-v)$. Using the same curvature domination $(u-v)^{\top}\Sigma_S(u-v) \leq (u-v)^{\top}\Sigma(u-v) \leq C_{K,R}V_K(u,v)$, we retain the same functional form $\text{Var}(Z) \leq \frac{1}{2\gamma^2} + \frac{C_{\text{mask}}}{\gamma}V_K(u,v)$ with a possibly larger constant $C_{\text{mask}} \geq 1$ that depends only on $\int ||\omega||_2^2 d\mu(\omega)$ and R, but not on (x, x', L, Γ) . Frequencies ω are drawn from a spectral measure μ normalized such that $\mathbb{E}[||\omega||_2^2] = 1$, ensuring unit-variance random Fourier features and correct scaling under masking.

By construction of the encoding scheme in Subsection III-A and Bochner's identity for shift-invariant K (together with the $\sqrt{2/\gamma}$ scaling and the masking model) [47], we have the unbiasedness

$$\mathbb{E}[Z_j(x, x')] = K_{xx'} \quad \text{for all } x, x', \tag{49}$$

where the expectation is over (ω_j, b_j) . Moreover, since $|\cos(\cdot)| \leq 1$,

$$|\phi_j(x)| \le \sqrt{\frac{2}{\gamma}} \implies |Z_j(x, x')| = |\phi_j(x)\phi_j(x')| \le \frac{2}{\gamma}.$$
 (50)

Hence each $Z_j(x, x')$ is uniformly bounded by $b \triangleq 2/\gamma$.

Lemma 1 states that there exists $C_{\text{mask}} \geq 1$ and a bounded variance proxy $V_K(x, x')$ of the unmasked RFF estimator such that

$$\operatorname{Var}(Z_j(x, x')) \leq \frac{1}{2\gamma^2} + \frac{C_{\text{mask}}}{\gamma} V_K(x, x'). \tag{51}$$

Define $\sigma^2(x, x') \triangleq \text{Var}(Z_1(x, x'))$ for notational convenience. By independence of $\{Z_j\}_{j=1}^{m_k}$ across j,

$$\operatorname{Var}\left(\frac{1}{m_{k}} \sum_{j=1}^{m_{k}} Z_{j}(x, x')\right) = \frac{1}{m_{k}} \sigma^{2}(x, x') \leq \frac{1}{m_{k}} \left(\frac{1}{2\gamma^{2}} + \frac{C_{\text{mask}}}{\gamma} V_{K}(x, x')\right).$$

Let

$$\Delta_k(x, x') \triangleq \widetilde{K}_k(x, x') - K_{xx'} = \frac{1}{m_k} \sum_{j=1}^{m_k} (Z_j(x, x') - \mathbb{E}Z_j(x, x'))$$

be the MC kernel error. For a fixed pair (x, x') and any t > 0, the scalar Bernstein inequality for i.i.d. zero-mean, bounded random variables (with bound $b = 2/\gamma$) yields

$$\mathbb{P}(|\Delta_k(x, x')| \ge t) \le 2 \exp\left(-\frac{m_k t^2}{2 \sigma^2(x, x') + \frac{2}{2} b t}\right).$$
 (52)

Using (51) and $b = 2/\gamma$, we get for all (x, x'),

$$\mathbb{P}(|\Delta_{k}(x, x')| \ge t) \le 2 \exp\left(-\frac{m_{k} t^{2}}{\frac{1}{\gamma^{2}} + \frac{2C_{\text{mask}}}{\gamma} V_{K}(x, x') + \frac{4}{3\gamma} t}\right).$$
 (53)

For any $\delta' \in (0,1)$, choose the deviation

$$t(x, x'; \delta') \triangleq \sqrt{\frac{2}{m_k} \left(\frac{1}{2\gamma^2} + \frac{C_{\text{mask}}}{\gamma} V_K(x, x')\right) \log \frac{2}{\delta'}} + \frac{4}{3\gamma m_k} \log \frac{2}{\delta'}.$$
 (54)

Plugging (54) into (53) shows that for each fixed pair (x, x').

$$\mathbb{P}(|\Delta_k(x,x')| \geq t(x,x';\delta')) \leq \delta'.$$

Therefore, with probability at least $1 - \delta'$ over the encoder randomness,

$$|\Delta_k(x, x')| \le t(x, x'; \delta')$$
 for that fixed (x, x') . (55)

Square both sides of (55) and integrate over (x, x') (w.r.t. the product law induced by \mathbb{P}_X and \mathbf{w}). Using $(a+b)^2 \leq 2a^2 + 2b^2$ and the boundedness of V_K (say $0 \leq V_K(x, x') \leq \overline{V}_K$), we obtain on the same probability event:

$$\mathbb{E}_{x,x'}[\Delta_k(x,x')^2] \leq \frac{4}{m_k} \mathbb{E}_{x,x'} \left[\left(\frac{1}{2\gamma^2} + \frac{C_{\text{mask}}}{\gamma} V_K(x,x') \right) \log \frac{2}{\delta'} \right] + \frac{32}{9} \cdot \frac{1}{\gamma^2 m_k^2} \left(\log \frac{2}{\delta'} \right)^2 \\
= \frac{2}{\gamma^2 m_k} \log \frac{2}{\delta'} + \frac{4C_{\text{mask}}}{\gamma m_k} \left(\mathbb{E}_{x,x'}[V_K(x,x')] \right) \log \frac{2}{\delta'} + \frac{32}{9} \cdot \frac{1}{\gamma^2 m_k^2} \left(\log \frac{2}{\delta'} \right)^2.$$
(56)

Since $m_k \geq 1$ and $\gamma \in (0, 1]$, the second line's last term is lower order and can be absorbed into the first two by renormalizing constants for all $\delta' \in (0, 1/2]$. Hence there exists an absolute constant $C'_1 > 0$ (depending only on $\mathbb{E}_{x,x'}[V_K(x,x')]$ and the numerical constants in the Bernstein bound) such that, with probability at least $1 - \delta'^1$,

$$\mathbb{E}_{x,x'}\left[\left(\widetilde{K}_k(x,x') - K(\mathbf{w}(x),\mathbf{w}(x'))\right)^2\right] \leq \left(\frac{2}{\gamma^2 m_k} + \frac{C_1'}{\gamma m_k}\right) \log \frac{2}{\delta'},\tag{57}$$

with C'_1 depending only on the kernel family (through $\mathbb{E}[V_K]$) and on C_{mask} via Lemma 1. This proves Lemma 2.

Appendix C

Proof of Lemma 3

Proof. For brevity, write $m(x) = F_k(x)$ as the k-th target subfunction to be estimated, and let $\Phi(x) = \Phi_k(x) \in \mathbb{R}^{m_k}$ denote its corresponding encoded feature vector. Here $\Phi(x)$ represents the output of the encoder associated with user k, capturing the encoded representation of x used for training, rather than the raw input or the subfunction itself.

Let the training data be $\{(x_i, y_i)\}_{i=1}^M$, where

$$y_i = m(x_i) + \varepsilon_i, \qquad \mathbb{E}[\varepsilon_i \mid x_i] = 0, \qquad \mathbb{E}[\varepsilon_i^2 \mid x_i] \le \sigma^2,$$

with $\{\varepsilon_i\}$ independent of $\{x_i\}$ and of the encoder randomness. This model justifies the variance term $\frac{\sigma^2 d_{\lambda}}{M}$ that appears in the quenched and annealed risk bounds of Theorems 1–2, as it captures the stochastic contribution of the label noise in the ridge-regression decomposition. Define the population feature covariance operator and cross-covariance vector as

$$G_k \triangleq \mathbb{E}[\Phi(X)\Phi(X)^{\top}] \in \mathbb{R}^{m_k \times m_k}, \qquad g_k \triangleq \mathbb{E}[\Phi(X) m(X)] \in \mathbb{R}^{m_k}.$$
 (58)

where the expectation is taken with respect to the distribution of encoded inputs X (for a fixed assignment in the quenched setting, or averaged over the random ensemble in the annealed setting).

 $^{^{1}}$ Here the probability is taken with respect to the encoder randomness only, conditional on the fixed data distribution and the assignment topology (A, L).

We assume G_k is positive semidefinite (PSD) [48]. The population best linear predictor (BLP) in the feature space is any solution

$$\beta^{\star} \in \operatorname{Argmin}_{\beta \in \mathbb{R}^{m_k}} \mathbb{E}[(\Phi(X)^{\top}\beta - m(X))^2] \iff G_k \beta^{\star} = g_k,$$
 (59)

where we choose the minimum-norm solution if G_k is not invertible. The corresponding approximation error is

$$\mathcal{A} \triangleq \inf_{\beta} \mathbb{E}[(\Phi^{\top}\beta - m)^2] = \mathbb{E}[m^2] - g_k^{\top} G_k^{\dagger} g_k, \tag{60}$$

with G_k^{\dagger} the Moore–Penrose pseudoinverse. Let $\lambda > 0$. The population ridge solution is

$$\beta_{\lambda} \triangleq (G_k + \lambda I)^{-1} q_k. \tag{61}$$

Let $Z \in \mathbb{R}^{M \times m_k}$ be the design matrix with *i*th row $\Phi(x_i)^{\top}$, and $y = (y_1, \dots, y_M)^{\top}$. The (empirical) ridge estimator is

$$\widehat{\beta} \triangleq \operatorname{Argmin}_{\beta} \frac{1}{M} \|Z\beta - y\|_{2}^{2} + \lambda \|\beta\|_{2}^{2} = (S + \lambda I)^{-1} s, \quad S \triangleq \frac{1}{M} Z^{\top} Z, \quad s \triangleq \frac{1}{M} Z^{\top} y. \tag{62}$$

We analyze the population prediction risk of $\widehat{F}(x) = \widehat{\beta}^{\top} \Phi(x)$:

$$\mathcal{R}(\widehat{\beta}) \triangleq \mathbb{E}_X[(\Phi(X)^{\top}\widehat{\beta} - m(X))^2].$$

For any β , using $G_k \beta^* = g_k$,

$$\mathcal{R}(\beta) = \mathbb{E}[(\Phi^{\top}\beta - m)^{2}] = \mathbb{E}[(\Phi^{\top}(\beta - \beta^{\star}) + \Phi^{\top}\beta^{\star} - m)^{2}]$$

$$= \mathbb{E}[(\Phi^{\top}(\beta - \beta^{\star}))^{2}] + 2\mathbb{E}[(\Phi^{\top}(\beta - \beta^{\star}))(\Phi^{\top}\beta^{\star} - m)] + \mathbb{E}[(\Phi^{\top}\beta^{\star} - m)^{2}]. \tag{63}$$

The middle term vanishes:

$$\mathbb{E}[(\Phi^{\top}(\beta - \beta^{\star}))(\Phi^{\top}\beta^{\star} - m)] = (\beta - \beta^{\star})^{\top}(\mathbb{E}[\Phi\Phi^{\top}]\beta^{\star} - \mathbb{E}[\Phi m]) = (\beta - \beta^{\star})^{\top}(G_k\beta^{\star} - g_k) = 0.$$

Hence

$$\mathcal{R}(\beta) = \mathcal{A} + (\beta - \beta^*)^{\top} G_k(\beta - \beta^*). \tag{64}$$

In particular,

$$\mathcal{R}(\widehat{\beta}) = \mathcal{A} + (\widehat{\beta} - \beta^{\star})^{\mathsf{T}} G_k(\widehat{\beta} - \beta^{\star}). \tag{65}$$

Write

$$\widehat{\beta} - \beta^* = (\widehat{\beta} - \beta_{\lambda}) + (\beta_{\lambda} - \beta^*).$$

Using $(a+b)^{\top}G_k(a+b) \leq 2 a^{\top}G_ka + 2 b^{\top}G_kb$ for PSD G_k ,

$$(\widehat{\beta} - \beta^{\star})^{\top} G_k(\widehat{\beta} - \beta^{\star}) \leq 2 (\widehat{\beta} - \beta_{\lambda})^{\top} G_k(\widehat{\beta} - \beta_{\lambda}) + 2 (\beta_{\lambda} - \beta^{\star})^{\top} G_k(\beta_{\lambda} - \beta^{\star}).$$
(66)

Combining (65) and (66),

$$\mathcal{R}(\widehat{\beta}) \leq \mathcal{A} + 2(\widehat{\beta} - \beta_{\lambda})^{\top} G_{k}(\widehat{\beta} - \beta_{\lambda}) + 2(\beta_{\lambda} - \beta^{\star})^{\top} G_{k}(\beta_{\lambda} - \beta^{\star}). \tag{67}$$

We will bound the last two terms as "variance" and "regularization bias," respectively.

Since $G_k \beta^* = g_k$, the population ridge solution (61) satisfies

$$\beta_{\lambda} - \beta^{\star} = (G_k + \lambda I)^{-1} g_k - \beta^{\star} = (G_k + \lambda I)^{-1} G_k \beta^{\star} - \beta^{\star} = -\lambda (G_k + \lambda I)^{-1} \beta^{\star}$$

Therefore

$$(\beta_{\lambda} - \beta^{\star})^{\top} G_{k}(\beta_{\lambda} - \beta^{\star}) = \lambda^{2} \beta^{\star \top} (G_{k} + \lambda I)^{-1} G_{k} (G_{k} + \lambda I)^{-1} \beta^{\star}$$

$$= \lambda \beta^{\star \top} \left(\lambda (G_{k} + \lambda I)^{-1} \right) (G_{k} + \lambda I)^{-1} G_{k} \beta^{\star}$$

$$\leq \lambda \beta^{\star \top} (G_{k} + \lambda I)^{-1} G_{k} \beta^{\star} \leq \lambda \beta^{\star \top} G_{k} \beta^{\star}. \tag{68}$$

The first inequality uses $\lambda(G_k + \lambda I)^{-1} \leq I$ (PSD order); the second uses $(G_k + \lambda I)^{-1}G_k \leq I$. Now, invoking the standard source condition induced by the RKHS assumption $m \in \mathcal{H}_K$: there exists h in the closure of the linear span of features such that

$$m(\cdot) = \langle h, \Phi(\cdot) \rangle_{\mathcal{H}}, \qquad ||h||_{\mathcal{H}} \leq B,$$

which is equivalent (via (58)) to $g \in \text{Range}(G_k^{1/2})$ with

$$\|G_k^{-1/2}g_k\|_2 \le B. (69)$$

Since $G_k \beta^* = g_k$ and we take the minimum-norm solution, $G_k^{1/2} \beta^* = G_k^{-1/2} g_k$, hence

$$\beta^{\star \top} G_k \beta^{\star} = \|G_k^{1/2} \beta^{\star}\|_2^2 = \|G_k^{-1/2} g_k\|_2^2 \leq B^2.$$

Plugging in (68),

$$(\beta_{\lambda} - \beta^{\star})^{\top} G_k(\beta_{\lambda} - \beta^{\star}) \leq B^2 \lambda. \tag{70}$$

We now bound $\mathbb{E}[(\widehat{\beta} - \beta_{\lambda})^{\top} G_k(\widehat{\beta} - \beta_{\lambda})]$. By the normal equations (62),

$$(S + \lambda I)\widehat{\beta} = s,$$
 $(G_k + \lambda I)\beta_{\lambda} = g_k,$

hence

$$\widehat{\beta} - \beta_{\lambda} = (S + \lambda I)^{-1} \left(s - S\beta_{\lambda} - \lambda \beta_{\lambda} \right) = (S + \lambda I)^{-1} \left(\frac{1}{M} Z^{\top} (y - Z\beta_{\lambda}) \right). \tag{71}$$

Write the residual vector $r \in \mathbb{R}^M$ with entries

$$r_i \triangleq y_i - \Phi(x_i)^{\top} \beta_{\lambda} = (m(x_i) - \Phi(x_i)^{\top} \beta_{\lambda}) + \varepsilon_i.$$

By definition of β_{λ} , the population normal equation implies

$$\mathbb{E}[\Phi(X) (m(X) - \Phi(X)^{\top} \beta_{\lambda})] = g_k - G_k \beta_{\lambda} = \lambda \beta_{\lambda},$$

so conditionally on $\{x_i\}$ the mean of r is controlled, while the noise part has variance σ^2 . Now set $v \triangleq \hat{\beta} - \beta_{\lambda}$. From (71),

$$v = (S + \lambda I)^{-1} \left(\frac{1}{M} Z^{\top} (y - Z \beta_{\lambda}) \right).$$

Hence

$$v^{\top} G_k v = \frac{1}{M^2} (y - Z\beta_{\lambda})^{\top} Z (S + \lambda I)^{-1} G_k (S + \lambda I)^{-1} Z^{\top} (y - Z\beta_{\lambda})$$
$$= \frac{1}{M^2} \operatorname{tr} \left(Z (S + \lambda I)^{-1} G_k (S + \lambda I)^{-1} Z^{\top} (y - Z\beta_{\lambda}) (y - Z\beta_{\lambda})^{\top} \right),$$

where we used $u^{\top}Au = \operatorname{tr}(Auu^{\top})$.

Write $y - Z\beta_{\lambda} = (m - Z\beta_{\lambda}) + \varepsilon$, with $\mathbb{E}[\varepsilon] = 0$, $\mathbb{E}[\varepsilon \varepsilon^{\top}] = \sigma^{2}I_{M}$, and $\varepsilon \perp (Z, X)$. Conditioning on (Z, X) and taking expectation in ε ,

$$\mathbb{E}_{\varepsilon}[(y - Z\beta_{\lambda})(y - Z\beta_{\lambda})^{\top}] = \sigma^{2}I_{M} + (m - Z\beta_{\lambda})(m - Z\beta_{\lambda})^{\top}.$$

The deterministic second term contributes to the bias part already controlled above; keeping only the stochastic contribution gives the upper bound

$$\mathbb{E}[v^{\top}G_{k}v] \leq \frac{\sigma^{2}}{M^{2}} \mathbb{E}\Big[\operatorname{tr}\Big(Z(S+\lambda I)^{-1}G_{k}(S+\lambda I)^{-1}Z^{\top}\Big)\Big]$$

$$= \frac{\sigma^{2}}{M^{2}} \mathbb{E}\Big[\operatorname{tr}\Big(Z^{\top}Z(S+\lambda I)^{-1}G_{k}(S+\lambda I)^{-1}\Big)\Big] \qquad \text{(cyclicity of trace)}$$

$$= \frac{\sigma^{2}}{M} \mathbb{E}\Big[\operatorname{tr}\Big(S(S+\lambda I)^{-1}G_{k}(S+\lambda I)^{-1}\Big)\Big]$$

$$= \frac{\sigma^{2}}{M} \mathbb{E}\Big[\operatorname{tr}\Big(G_{k}(S+\lambda I)^{-1}S(S+\lambda I)^{-1}\Big)\Big].$$

Next, use the PSD order and the resolvent's operator monotonicity/convexity to pass from the empirical covariance $S = \frac{1}{M} Z^{\top} Z$ to its mean $G_k = \mathbb{E}[S]$:

$$\mathbb{E}\left[(S+\lambda I)^{-1}S(S+\lambda I)^{-1}\right] \leq (G_k+\lambda I)^{-1}G_k(G_k+\lambda I)^{-1}.$$

Therefore,

$$\mathbb{E}[v^{\top}G_k v] \leq \frac{\sigma^2}{M} \operatorname{tr} \left(G_k (G_k + \lambda I)^{-1} G_k (G_k + \lambda I)^{-1} \right)$$

$$\leq \frac{\sigma^2}{M} \operatorname{tr} \left(G_k (G_k + \lambda I)^{-1} \right),$$

since $(G_k + \lambda I)^{-1}G_k(G_k + \lambda I)^{-1} \leq (G_k + \lambda I)^{-1}$ (because $0 \leq G_k \leq G_k + \lambda I$). Recognizing the effective dimension $d_{\lambda,k} \triangleq \operatorname{tr}(G_k(G_k + \lambda I)^{-1})$ and allowing a universal constant C > 0 to absorb small fluctuation terms yields

$$\mathbb{E}\left[\left(\widehat{\beta} - \beta_{\lambda}\right)^{\top} G_{k}(\widehat{\beta} - \beta_{\lambda})\right] \leq C \frac{\sigma^{2}}{M} \operatorname{tr}\left(G_{k} \left(G_{k} + \lambda I\right)^{-1}\right) = C \frac{\sigma^{2}}{M} d_{\lambda,k}, \tag{72}$$

where $d_{\lambda,k} \triangleq \operatorname{tr}(G_k(G_k + \lambda I)^{-1})$ is the effective dimension, and C > 0 is an absolute constant. Taking expectation of (67) and using (70) and (72),

$$\mathbb{E}[\mathcal{R}(\widehat{\beta})] \leq \mathcal{A} + 2C \frac{\sigma^2}{M} d_{\lambda,k} + 2B^2 \lambda.$$

Renaming constants $C_2' = 2C$ and $C_3' = 2$ gives

$$\mathbb{E}_{x} \left[\left(\widehat{\beta}^{\top} \Phi(x) - m(x) \right)^{2} \right] \leq \underbrace{\inf_{\beta} \mathbb{E}_{x} \left[\left(\Phi^{\top} \beta - m \right)^{2} \right]}_{\text{approximation error } \mathcal{A}} + C_{2}' \frac{\sigma^{2} d_{\lambda, k}}{M} + C_{3}' B^{2} \lambda,$$

which is precisely (21). This completes the proof.

Appendix D

Proof of Lemma 4

Proof. Let ρ be the distribution of $U = \mathbf{w}(X) \in \mathbb{R}^L$ induced by $X \sim \mathbb{P}_X$. Consider the integral operator $T_K : L_2(\rho) \to L_2(\rho)$ defined by

$$(T_K f)(u) = \int K(u, v) f(v) d\rho(v).$$

By standard Mercer's theory [50], T_K is self-adjoint, positive, trace-class, and admits an orthonormal eigen-system $\{(\lambda_j, \varphi_j)\}_{j \geq 1}$ in $L_2(\rho)$ with nonincreasing eigenvalues $\lambda_1 \geq \lambda_2 \geq \cdots \geq 0$;

$$T_K \varphi_j = \lambda_j \varphi_j, \qquad \langle \varphi_i, \varphi_j \rangle_{L_2(\rho)} = \delta_{ij}.$$

The RKHS \mathcal{H}_K associated with K embeds continuously into $L_2(\rho)$ and every $f \in \mathcal{H}_K$ has an expansion

$$f = \sum_{j>1} \alpha_j \varphi_j, \qquad ||f||_{L_2(\rho)}^2 = \sum_{j>1} \alpha_j^2, \qquad ||f||_{\mathcal{H}_K}^2 = \sum_{j>1} \frac{\alpha_j^2}{\lambda_j}.$$

The ball constraint $F_k \in \mathcal{H}_K$ with $||F_k||_{\mathcal{H}_K} \leq B$ therefore means that its coefficients (α_j) satisfy

$$\sum_{j>1} \frac{\alpha_j^2}{\lambda_j} \le B^2.$$

Any measurable encoder/decoder that outputs at most m scalars per input induces a reconstruction map

$$\mathcal{R}: \mathcal{H}_K \longrightarrow \mathcal{G}_m \subset L_2(\rho),$$

¹A direct derivation uses (71), the identity $\mathbb{E}\left[\frac{1}{M}Z^{\top}\varepsilon\varepsilon^{\top}Z\right] = \frac{\sigma^2}{M}G_k$ (with $\varepsilon = (\varepsilon_i)$ independent of Z), and the PSD bound $(S + \lambda I)^{-1}S(S + \lambda I)^{-1} \leq (G + \lambda I)^{-1}G(G + \lambda I)^{-1}$ in expectation (via Jensen/monotonicity of the resolvent), then take traces to arrive at $\frac{\sigma^2}{M} \operatorname{tr}[G(G + \lambda I)^{-1}]$. Any additional sample-covariance fluctuation is absorbed into C [49].

whose range \mathcal{G}_m has at most m degrees of freedom in $L_2(\rho)$ (informally, the decoder can only move inside an m-dimensional manifold because it receives only m real numbers; formally, one can show the image is contained in the closure of some m-dimensional linear subspace).¹

Hence, for the purpose of a lower bound, it suffices to consider linear reconstructions from an m-dimensional subspace $V_m \subset L_2(\rho)$:

$$\widehat{f} = P_{V_m}(f),$$

where P_{V_m} is the $L_2(\rho)$ -orthogonal projector onto V_m .

Fix an m-dimensional subspace V_m . Write V_m^{\perp} for its $L_2(\rho)$ -orthogonal complement. For $f = \sum_j \alpha_j \varphi_j \in \mathcal{H}_K$, the squared L_2 reconstruction error is

$$||f - P_{V_m} f||_{L_2(\rho)}^2 = ||P_{V_m^{\perp}} f||_{L_2(\rho)}^2.$$

The worst-case (squared) error over the RKHS ball $\{f: ||f||_{\mathcal{H}_K} \leq B\}$ is

$$\sup_{\|f\|_{\mathcal{H}_{K}} \leq B} \ \|P_{V_{m}^{\perp}} f\|_{L_{2}(\rho)}^{2} \ = \ B^{2} \cdot \sup_{\sum_{j} \alpha_{j}^{2} / \lambda_{j} \leq 1} \ \left\|P_{V_{m}^{\perp}} \sum_{j} \alpha_{j} \varphi_{j} \right\|_{L_{2}(\rho)}^{2}.$$

Let $\{\psi_i\}_{i\geq 1}$ be any orthonormal basis that diagonalizes simultaneously T_K and the projector $P_{V_m^{\perp}}$ (this can be done by choosing V_m as a span of some eigenfunctions). For now, expand $P_{V_m^{\perp}}\varphi_j$ in the $\{\varphi_j\}$ basis. By Pythagoras and the orthogonality of $\{\varphi_j\}$,

$$\|P_{V_m^{\perp}}f\|_{L_2}^2 \ = \ \sum_{j \geq 1} \alpha_j^2 \, \|P_{V_m^{\perp}}\varphi_j\|_{L_2}^2, \qquad 0 \leq \|P_{V_m^{\perp}}\varphi_j\|_{L_2}^2 \leq 1.$$

Thus we need to maximize $\sum_j \alpha_j^2 \theta_j$ subject to $\sum_j \alpha_j^2 / \lambda_j \leq 1$, where $\theta_j = \|P_{V_m^{\perp}} \varphi_j\|_{L_2}^2 \in [0, 1]$ encodes how much of eigen-direction j lies outside V_m .

By Cauchy–Schwarz, the maximizer concentrates all mass on the coordinates with the largest ratio $\theta_i \lambda_i$. Hence

$$\sup_{\sum_{j}\alpha_{j}^{2}/\lambda_{j}\leq 1}\ \sum_{j}\alpha_{j}^{2}\theta_{j}\ =\ \max_{j\geq 1}\ \theta_{j}\lambda_{j}.$$

However, because V_m is m-dimensional, one can make at most m values of θ_j equal to 0 (those directions that V_m fully captures), while all remaining directions have $\theta_j = 1$ (completely outside V_m). Thus, for any m-dimensional V_m ,

$$\sup_{\|f\|_{\mathcal{H}_K} \leq B} \ \|P_{V_m^{\perp}} f\|_{L_2}^2 \ \geq \ B^2 \cdot \max_{j > m} \lambda_j.$$

¹Formally, by classical results on Kolmogorov m-widths in Hilbert spaces [51, Thm. 1.3.2], [52, Cor. 2.3.2], see also [53, Thm. 4.4], the worst-case L_2 -error for approximating the RKHS ball using at most m real scalars is minimized by linear reconstruction from an m-dimensional subspace, namely the span of the top-m eigenfunctions of T_K . Hence restricting to linear m-dimensional reconstructions is without loss for a minimax lower bound.

This bound is correct but not yet tight; we can do better by the next step. In particular, we optimize over the choice of V_m . The optimal V_m for approximating the RKHS ball in L_2 is the span of the top m eigenfunctions:

$$V_m^{\star} = \operatorname{span}\{\varphi_1, \dots, \varphi_m\}.$$

For this choice, $P_{V_m^{\star\perp}}\varphi_j=\varphi_j$ for j>m and 0 otherwise, hence

$$\|P_{V_m^{\star\perp}}f\|_{L_2}^2 \ = \ \sum_{j>m} \alpha_j^2.$$

Subject to $\sum_{j} \alpha_{j}^{2}/\lambda_{j} \leq B^{2}$, the worst case is when all the RKHS budget is spent on the tail coordinates j > m, aligned proportionally to λ_{j} :

$$\alpha_j^2 = B^2 \lambda_j \cdot \mathbb{I}\{j > m\}.$$

Therefore,

$$\sup_{\|f\|_{\mathcal{H}_K} \leq B} \ \|f - P_{V_m^\star} f\|_{L_2}^2 \ = \ \sup_{\sum_j \alpha_j^2/\lambda_j \leq B^2} \ \sum_{j > m} \alpha_j^2 \ = \ B^2 \sum_{j > m} \lambda_j.$$

Moreover, a standard Kolmogorov width argument shows that no other m-dimensional subspace can do better (the tail-sum is the optimal worst-case squared error).

As argued before, any scheme that communicates at most m scalars per input cannot achieve smaller worst-case L_2 error than the best m-dimensional linear projector. Hence

$$\inf_{\text{schemes with } \leq m \text{ scalars }} \sup_{\|f\|_{\mathcal{H}_K} \leq B} \mathbb{E}_x \big[(\widehat{f}(x) - f(x))^2 \big] \geq \inf_{\dim(V_m) = m} \sup_{\|f\|_{\mathcal{H}_K} \leq B} \|f - P_{V_m} f\|_{L_2(\rho)}^2.$$

By the above, the right-hand side equals $B^2 \sum_{j>m} \lambda_j$, attained by choosing $V_m = V_m^*$ and is therefore the minimax lower bound. Applying the bound to the ball $\{f \in \mathcal{H}_K : ||f||_{\mathcal{H}_K} \leq B\}$ that contains F_k , we obtain for any m-scalar scheme:

$$\mathbb{E}_x[\|\widehat{F}_k(x) - F_k(x)\|_2^2] \geq B^2 \sum_{j>m} \lambda_j.$$

This proves the lemma.

Appendix E

Proof of Lemma 5

Proof. By assumption, no server that links to user k ever computes coordinate ℓ^* . Thus, for any encoder family (measurable functions of the assigned subfunction outputs), the random symbol stream routed to user k depends only on the coordinates in $[L] \setminus \{\ell^*\}$. Since these coordinates are identical for x_0 and x_1 , we have the equality in distribution

$$\mathcal{R}_k(x_0) \stackrel{d}{=} \mathcal{R}_k(x_1), \tag{73}$$

where $\mathcal{R}_k(\cdot)$ denotes the full collection of real scalars received by user k (over all linked servers and shots), including any encoder randomness. Consequently, for any (possibly randomized) decoder ψ_k ,

$$\widehat{F}_k(x_0) = \psi_k(\mathcal{R}_k(x_0)) \stackrel{d}{=} \psi_k(\mathcal{R}_k(x_1)) = \widehat{F}_k(x_1).$$

That is, the distribution of the estimator's output is the same under x_0 and x_1 ; the observation model cannot distinguish the two inputs.

Consider the auxiliary (least favorable) prior Π on inputs supported on $\{x_0, x_1\}$ with equal mass:

$$X \sim \frac{1}{2}\delta_{x_0} + \frac{1}{2}\delta_{x_1}.$$

Let \hat{F}_k be any estimator (any encoder/decoder scheme). The Bayes mean-squared error under Π is

$$\mathcal{B} \triangleq \mathbb{E}_{X \sim \Pi} [\|\widehat{F}_k(X) - F_k(X)\|_2^2] = \frac{1}{2} \mathbb{E} [\|\widehat{F}_k(x_0) - F_k(x_0)\|_2^2] + \frac{1}{2} \mathbb{E} [\|\widehat{F}_k(x_1) - F_k(x_1)\|_2^2],$$

where the expectation is over the encoder/decoder randomness.

By (73), $\hat{F}_k(x_0)$ and $\hat{F}_k(x_1)$ have the same distribution. Let Z be a random variable with this common distribution (a version of the estimator's output under either hypothesis). Then

$$\mathcal{B} = \frac{1}{2} \mathbb{E} [\|Z - F_k(x_0)\|_2^2] + \frac{1}{2} \mathbb{E} [\|Z - F_k(x_1)\|_2^2].$$

Using the parallelogram identity, the function $z\mapsto \frac{1}{2}\|z-a\|_2^2+\frac{1}{2}\|z-b\|_2^2$ is minimized at z=(a+b)/2 with minimum value $\|a-b\|_2^2/4$. Therefore, for any distribution of Z,

$$\mathcal{B} \geq \frac{1}{4} \|F_k(x_0) - F_k(x_1)\|_2^2 = \frac{\Delta_{\star}^2}{4}. \tag{74}$$

This is the standard Le Cam two-point lower bound in squared loss, specialized to the case where the observation laws coincide (total variation distance zero), which forces the Bayes risk to be the midpoint error. The frequentist risk of any estimator under the original data distribution \mathbb{P}_X is $\mathbb{E}_{x \sim \mathbb{P}_X}[\|\widehat{F}_k(x) - F_k(x)\|_2^2]$. Since the Bayes risk lower bounds the minimax risk, and in particular the risk under any fixed scheme for some input distribution, we obtain the universal lower bound

$$\inf_{\text{all schemes}} \sup_{\text{priors on } \{x_0, x_1\}} \mathbb{E}[\|\widehat{F}_k(X) - F_k(X)\|_2^2] \geq \frac{\Delta_{\star}^2}{4}.$$

Hence, there exists a (scheme-independent) constant

$$\varepsilon_{\text{cov},k}(\mathsf{A},\mathsf{L}) \triangleq \frac{\Delta_{\star}^2}{4} > 0$$
 (75)

such that the mean-squared error cannot be smaller than $\varepsilon_{\text{cov},k}(\mathsf{A},\mathsf{L})$ whenever the observation model leaves ℓ^* completely unobserved for user k. This proves the lemma as stated.

If \mathbb{P}_X is fixed and absolutely continuous, one can localize the argument: by continuity of F_k along the ℓ^* -direction and essential dependence, there exist disjoint measurable neighborhoods U_0, U_1 around x_0, x_1 with positive masses $q_0, q_1 > 0$ and such that

$$\inf_{x \in U_0, \ x' \in U_1} \|F_k(x) - F_k(x')\|_2 \ge \frac{\Delta_{\star}}{2}.$$

Moreover, since no linked server observes ℓ^* , the conditional law of $\mathcal{R}_k(X)$ given $X \in U_0$ equals that given $X \in U_1$ (they depend only on the other coordinates, which we fix by shrinking U_0, U_1 if necessary). Conditioning on $X \in U_0 \cup U_1$ and repeating the two-point argument yields the frequentist lower bound

$$\mathbb{E}_{x \sim \mathbb{P}_X} \left[\| \widehat{F}_k(x) - F_k(x) \|_2^2 \right] \geq \frac{q_0 + q_1}{2} \cdot \frac{(\Delta_{\star}/2)^2}{1} = \frac{(q_0 + q_1) \Delta_{\star}^2}{8} =: \varepsilon_{\text{cov},k}(\mathsf{A},\mathsf{L}) > 0.$$

Either way, $\varepsilon_{\text{cov},k}(\mathsf{A},\mathsf{L})$ depends only on the separation Δ_{\star} (and, for the localized version, on the local masses q_0, q_1), and is independent of the scheme.

Appendix F

Proof of Proposition 1

Proof. Note that, per user, the total fraction of effective feature dimensions retained by the decoder equals

$$m_{\text{eff}} \triangleq \min \left\{ 1, \ \frac{T \gamma N}{K} \right\}, \qquad \kappa \triangleq 1 - m_{\text{eff}}.$$
 (76)

Here m_{eff} is the kept fraction of spectral mass and κ is the discarded fraction. In the limit considered below, κm_k is the lower-tail spectral mass that contributes to the error. Fix a user k and set $\Phi \equiv \Phi_k$, $m(\cdot) \equiv F_k(\cdot)$. Define

$$G \triangleq \mathbb{E}[\Phi(X)\Phi(X)^{\top}] \in \mathbb{R}^{m_k \times m_k}, \qquad g \triangleq \mathbb{E}[\Phi(X) m(X)] \in \mathbb{R}^{m_k}.$$

These are exactly the objects of Lemma 3 (Eq. (58)). Let $\widehat{F}_{M,\lambda}(x) = \widehat{\beta}_{M,\lambda}^{\mathsf{T}} \Phi(x)$ be the ridge predictor, and recall the risk decomposition (see Eq. (21) with $\sigma^2 = 0$):

$$\mathbb{E}[(\widehat{F}_{M,\lambda}(X) - m(X))^2] \leq \inf_{\beta} \mathbb{E}[(\beta^{\top} \Phi(X) - m(X))^2] + C_3' B^2 \lambda. \tag{77}$$

As $M \to \infty$, the sample covariance/second moment $S = \frac{1}{M}Z^{\top}Z$ and $s = \frac{1}{M}Z^{\top}y$ converge almost surely to G and g (law of large numbers), hence the empirical ridge solution $\widehat{\beta}_{M,\lambda} = (S + \lambda I)^{-1}s$ converges to the population ridge solution

$$\beta_{\lambda} = (G + \lambda I)^{-1} g. \tag{78}$$

Therefore, for each fixed $\lambda > 0$,

$$\widehat{F}_{M,\lambda}(x) \xrightarrow{L_2(\mathbb{P}_X)} F_{\lambda}(x) := \beta_{\lambda}^{\top} \Phi(x),$$

and (77) gives $\mathbb{E}[(F_{\lambda}(X) - m(X))^2] \leq A + C_3'B^2\lambda$. Let β^* be any population best linear predictor (BLP), i.e. a minimum-norm solution of $G\beta = g$ (Eq. (59)). Standard resolvent continuity yields

$$\beta_{\lambda} = (G + \lambda I)^{-1} g \xrightarrow{\lambda \downarrow 0} G^{\dagger} g =: \beta^{\star}, \tag{79}$$

where G^{\dagger} is the Moore–Penrose pseudoinverse. Consequently,

$$F_{\lambda} = \beta_{\lambda}^{\top} \Phi \xrightarrow{L_2(\mathbb{P}_X)} F^{\star} := (\beta^{\star})^{\top} \Phi.$$

By (77) with $M = \infty$ and letting $\lambda \downarrow 0$,

$$\lim_{\lambda \downarrow 0} \mathbb{E}[(F_{\lambda}(X) - m(X))^{2}] \leq \mathcal{A},$$

and since F^* attains the BLP, $\mathbb{E}[(F^*(X) - m(X))^2] = \mathcal{A}$. Introduce the linear operator $J : \mathbb{R}^{m_k} \to L_2(\mathbb{P}_X)$ defined by

$$(J\beta)(\cdot) = \beta^{\top} \Phi(\cdot).$$

A direct computation shows $J^*J = G$ and $J^*m = g$ (cf. (58)). The function predicted by ridge at parameter λ is

$$F_{\lambda} = J\beta_{\lambda} = J(G + \lambda I)^{-1}g = J(G + \lambda I)^{-1}J^{*}m.$$

Let $P_{\lambda} \triangleq J(G + \lambda I)^{-1}J^* : L_2(\mathbb{P}_X) \to L_2(\mathbb{P}_X)$. Then $F_{\lambda} = P_{\lambda}m$. Using (79), the zero-penalty limit is

$$P \triangleq \lim_{\lambda \downarrow 0} P_{\lambda} = J G^{\dagger} J^*.$$

We claim that P is the orthogonal projector onto the closed subspace $V \triangleq \overline{\mathrm{Range}(J)} = \overline{\mathrm{span}\{\Phi(\cdot)\}}$. Indeed:

- P is self-adjoint: $P^* = J G^{\dagger} J^* = P$ since G^{\dagger} is symmetric.
- $P^2=JG^\dagger J^*JG^\dagger J^*=JG^\dagger GG^\dagger J^*=JG^\dagger J^*=P$ because $G^\dagger GG^\dagger=G^\dagger J^*=G^\dagger J^*=G$
- Range(P) \subseteq Range(J) since $P = J(\cdot)$; conversely, for any $h \in \text{Range}(J)$, $h = J\beta$, so $Ph = JG^{\dagger}J^{*}J\beta = JG^{\dagger}G\beta = J\Pi_{\text{Range}(G)}\beta$, which lies in Range(J) and equals h if $\beta \in \text{Range}(G)$ (and the closure gives the whole V). Hence Range(P) = V.

Thus P is the orthogonal projector onto V, and

$$\widehat{F}_{M,\lambda} \xrightarrow[M \to \infty, \lambda \downarrow 0]{L_2(\mathbb{P}_X)} Pm.$$

By orthogonality of P,

$$\lim_{M \to \infty, \ \lambda \downarrow 0} \mathbb{E}[(\widehat{F}_{M,\lambda}(X) - m(X))^2] = \|(I - P)m\|_{L_2(\mathbb{P}_X)}^2.$$

In our linear/isotropic specialization we compare against linear targets of the form $m(\cdot) = u^{\top}w(\cdot)$ and, more generally, against K outputs aggregated as in (36). Averaging over an orthonormal basis of such linear targets (or, equivalently, taking the trace with respect to the induced covariance) yields that the aggregated projector loss equals the discarded first spectral moment of the Gram operator G:

$$\frac{1}{L} \sum_{\text{outputs}} \| (I - P) m \|_{L_2}^2 = \frac{1}{L} \operatorname{tr} ((I - P) J J^*) = \frac{1}{L} \operatorname{tr} ((I - \Pi) G), \tag{80}$$

where Π is the (matrix) projector in feature space that corresponds to P through J. Under the (Γ, Δ, T) budgets, only a fraction $m_{\text{eff}} = \frac{T\gamma N}{K}$ of feature-space degrees of freedom can be effectively retained; this is a rank constraint on Π :

$$\operatorname{rank}(\Pi) \leq m_{\text{eff}} m_k \iff \text{at least } \kappa m_k \text{ eigen-directions are discarded}, \ \kappa = 1 - m_{\text{eff}}.$$

By Ky Fan's maximum principle [54], among all rank-r projectors, the choice that minimizes $\operatorname{tr}((I-\Pi)G)$ keeps the top r eigenvectors of G. Hence the minimum discarded energy at rank $r=(1-\kappa)m_k$ equals the sum of the smallest κm_k eigenvalues. Writing the eigenvalues in ascending order $\xi_{(1)} \leq \cdots \leq \xi_{(m_k)}$, we have

$$\min_{\Pi: \Pi^2 = \Pi, \operatorname{rank}(\Pi) \le (1 - \kappa) m_k} \operatorname{tr}((I - \Pi)G) = \sum_{i=1}^{\lceil \kappa m_k \rceil} \xi_{(i)}.$$

Dividing by L and recalling (7),(37) yields the first equality in (39). Finally, for any empirical spectral law $\mu = \frac{1}{m_k} \sum_{i=1}^{m_k} \delta_{\xi_{(i)}}$, the lower-tail quantile identity (Hardy–Littlewood rearrangement; see Eq. (82)) gives

$$\frac{1}{m_k} \sum_{i=m_k-\lceil \kappa m_k \rceil+1}^{m_k} \xi_{(i)} = \int_0^{\kappa} Q_{\mu}^{\downarrow}(u) du,$$

and multiplying by $\frac{m_k}{L}$ (absorbed into the paper's normalization) yields the second equality in (39). We have shown: (i) $\widehat{F}_{M,\lambda} \to Pm$ with $P = JG^{\dagger}J^*$ the orthogonal projector onto $\overline{\text{span}\{\Phi(\cdot)\}}$; (ii) the aggregated L_2 risk equals the projector's discarded spectral mass; (iii) under the effective-rank budget, the discarded mass equals the sum of the smallest κm_k eigenvalues of G, equivalently the lower-tail quantile integral. This proves the proposition.

Appendix G

Proof of Theorem 3

Proof. Let μ be any probability law on $[0, \infty)$ with CDF F_{μ} and lower quantile $Q_{\mu}^{\downarrow}(u) = \inf\{x : F_{\mu}(x) \geq u\}$. The Hardy–Littlewood rearrangement identity gives, for every $t \in \mathbb{R}$,

$$\int x \, \mathbf{1}_{\{x \le t\}} \, d\mu(x) = \int_0^{F_\mu(t)} Q_\mu^{\downarrow}(u) \, du. \tag{81}$$

For discrete $\mu = \frac{1}{L} \sum_{i=1}^{L} \delta_{\xi_{(i)}}$ with ordered eigenvalues $\xi_{(1)} \geq \cdots \geq \xi_{(L)}$, one has $Q_{\mu}^{\downarrow}(u) = \xi_{(L-\lfloor uL \rfloor)}$ for $u \in [0,1]$, which provides the exact correspondence between the ordered eigenvalues and their quantile function. For any integer $q \in \{0,\ldots,L\}$,

$$\int_0^{q/L} Q_{\mu}^{\downarrow}(u) \, du = \frac{1}{L} \sum_{i=L-q+1}^L \xi_{(i)}. \tag{82}$$

Taking $q = \lceil \kappa L \rceil$ yields the expression for $D_{\text{MUDC}}^{\text{q}}$ stated above the theorem. For convenience, define the truncated first moment (lower-tail spectral mass)

$$\Phi_{\kappa}(\mu) \triangleq \int_0^{\kappa} Q_{\mu}^{\downarrow}(u) \, du,$$

which is monotone in κ and equals the normalized sum of the κL smallest eigenvalues when μ is empirical.

Let t satisfy $F_{\text{MP},\lambda'}(t) = \kappa$. Applying (81) to $\mu = \mu_{\text{A},\text{L}}$ at its κ -quantile and to $\mu = \text{MP}_{\lambda'}$ at threshold t gives

$$D_{\mathrm{MUDC}}^{\mathrm{q}} = \int_{0}^{\kappa} Q_{\mu_{\mathsf{A},\mathsf{L}}}^{\downarrow}(u) \, du, \qquad \Phi_{\mathrm{MP},\lambda'}(\kappa) = \int_{0}^{\kappa} Q_{\mathrm{MP},\lambda'}^{\downarrow}(u) \, du.$$

Subtracting the two yields (43).

Under a (Γ, Δ) -regular topology (A, L), each server computes exactly Γ subfunctions and transmits to exactly Δ users. The total feature budget implies that each user receives only a fraction $m_{\text{eff}} = \frac{T\gamma N}{K}$ of the full feature mass, so at least $\kappa = 1 - m_{\text{eff}}$ of the smallest eigen-directions must be discarded. Meanwhile, the normalized trace of the user Gram G_k —the average eigenvalue—is fixed by isotropy. Hence all feasible spectra share the same mean but differ in how that energy is distributed across eigen-directions.

Each G_k is a sum of N positive semidefinite contributions from the servers. When computation and link supports overlap, these block contributions are linearly dependent, concentrating energy in fewer principal directions and pushing some eigenvalues toward 0. Disjoint and balanced supports (the TDC configuration) correspond to orthogonal blocks whose contributions are nearly independent and spread energy as evenly as possible.

Since each G_k is Hermitian with fixed trace, write $\boldsymbol{\mu} = (\mu_1 \leq \cdots \leq \mu_L)$ and $\boldsymbol{\mu}^{\text{TDC}} = (\mu_1^{\text{TDC}} \leq \cdots \leq \mu_L)$ for the eigenvalues sorted in ascending order. We say $\boldsymbol{x} \prec \boldsymbol{y}$ (majorization) if $\sum_{i=1}^r x_i \leq \sum_{i=1}^r y_i$ for all $r = 1, \ldots, L$ and equality for r = L. Under the (Γ, Δ) budgets, any feasible G_k satisfies $\boldsymbol{\mu} \prec \boldsymbol{\mu}^{\text{TDC}}$.

For vectors sorted ascending, the map $S_s(\boldsymbol{x}) = \sum_{i=1}^s x_i$ is Schur-convex. Therefore, if $\boldsymbol{x} \prec \boldsymbol{y}$ then $\sum_{i=1}^s x_i \leq \sum_{i=1}^s y_i$ for all s. Applying this to the eigenvalue vectors of G_k and G_k^{TDC} with $s = \lfloor \kappa m_k \rfloor$ yields

$$\frac{1}{m_k} \sum_{i=1}^{\lfloor \kappa m_k \rfloor} \mu_i \leq \frac{1}{m_k} \sum_{i=1}^{\lfloor \kappa m_k \rfloor} \mu_i^{\text{TDC}}, \quad \text{i.e.,} \quad \Phi_{\kappa}(\mu) \leq \Phi_{\kappa}(\mu^{\text{TDC}}).$$

Equivalently, the partial-sum vector $(S_s(\boldsymbol{\mu}))_{s\leq L}$ lies below $(S_s(\boldsymbol{\mu}^{\text{TDC}}))_{s\leq L}$, confirming that the TDC topology minimizes the lower-tail spectral deficit and thus maximizes $\Phi_{\kappa}(\mu)$ among feasible configurations.

Under the linear/isotropic model $w(X) \sim (0, I_L)$, TDC ensures that the rows of each user's feature matrix are disjoint and balanced. Consequently, $G_k = E_k E_k^{\mathsf{T}}$ is (asymptotically) a random covariance (Wishart) matrix whose empirical spectral distribution converges to the Marchenko-Pastur law $MP_{\lambda'}$ with aspect ratio

$$\lambda' = \frac{\Delta}{\Gamma} = \frac{\delta K}{\gamma L}, \quad \text{support } [(1 - \sqrt{\lambda'})^2, (1 + \sqrt{\lambda'})^2].$$

Therefore the TDC limit satisfies

$$\mu^{\mathrm{TDC}} \Rightarrow \mathrm{MP}_{\lambda'}, \qquad \Phi_{\kappa}(\mu^{\mathrm{TDC}}) \to \Phi_{\mathrm{MP},\lambda'}(\kappa) = \int_0^{\kappa} Q_{\mathrm{MP},\lambda'}^{\downarrow}(u) \, du.$$

The convergence holds almost surely in the sense of weak convergence of empirical spectral distributions, i.e., $\frac{1}{L} \sum_i f(\xi_i^{\text{TDC}}) \to \int f(x) d\text{MP}_{\lambda'}(x)$ for every bounded continuous test function f. In particular, the associated quantile integrals converge, hence for any feasible topology (A, L),

$$\Phi_{\kappa}(\mu_{\mathsf{A},\mathsf{L}}) \leq \Phi_{\kappa}(\mu^{\mathsf{TDC}}) = \Phi_{\mathsf{MP},\lambda'}(\kappa).$$
(83)

Define the quenched MP-gap as

$$G^{\mathrm{q}}(\mathsf{A},\mathsf{L}) \triangleq \Phi_{\mathrm{MP},\lambda'}(\kappa) - \Phi_{\kappa}(\mu_{\mathsf{A},\mathsf{L}}) = \int_{0}^{\kappa} (Q_{\mathrm{MP},\lambda'}^{\downarrow}(u) - Q_{\mu_{\mathsf{A},\mathsf{L}}}^{\downarrow}(u)) du.$$

Since $Q_{\text{MP},\lambda'}^{\downarrow}(u) \geq Q_{\mu_{\text{A},\text{L}}}^{\downarrow}(u)$ for Lebesgue-a.e. $u \in [0,\kappa]$, the integrand is nonnegative almost everywhere, giving

$$G^{\mathbf{q}}(\mathsf{A},\mathsf{L}) \ge 0. \tag{84}$$

Equality in (84) holds iff $Q_{\mu_{A,L}}^{\downarrow}(u) = Q_{\text{MP},\lambda'}^{\downarrow}(u)$ for almost every $u \in [0, \kappa]$, i.e., when the two spectral laws coincide on the lower-tail region.

More quantitatively, if there exists $\alpha > 0$ and a measurable subset $U \subset [0, \kappa]$ of Lebesgue measure $|U| = \eta > 0$ such that

$$Q_{\mu_{\mathsf{A},\mathsf{L}}}^{\downarrow}(u) \le Q_{\mathrm{MP},\lambda'}^{\downarrow}(u) - \alpha, \quad \forall u \in U,$$

then integrating over U yields the explicit inequality

$$G^{\mathbf{q}}(\mathsf{A},\mathsf{L}) \geq \int_{U} \left(Q_{\mathsf{MP},\lambda'}^{\downarrow}(u) - Q_{\mu_{\mathsf{A},\mathsf{L}}}^{\downarrow}(u) \right) du \geq \alpha \, \eta, \tag{85}$$

providing a quantitative lower bound on the gap proportional to the mean separation of the quantile curves over any region of persistent spectral deficit.

